The University of Edinburgh

School of Engineering

Institute for Infrastructure and Environment

Academic Year 2014-2015

The Effect of Oxygen Mass Flux and Flow Velocity on Forward Smouldering

Student: Carmen Gorska Putynska

Promoter: Dr Rory Hadden

Master thesis submitted in the Erasmus Mundus Study Programme

International Master of Science in Fire Safety Engineering

30 April 2015 Read and approved

ABSTRACT

The aim of this work is to understand better the behaviour and characteristics of a phenomena called "smouldering combustion". This is a specific form of burning in condensed-phase fuels, it is flameless and with lower temperatures and burning rates compared to flaming combustion.

Even if the nature of smouldering looks weak it actually creates a serious fire hazard. On one hand, the products of the combustion are very rich in toxic gases, this leads to deaths in residential fires. On the other hand, smouldering can start with very small heat sources and later evolve into flaming that can cause huge wildfires areas and other disasters. Sadly smouldering is often devaluated in the fire safety communities.

This work presents the information extracted from a matrix of peat mixed with sand that is taken into smouldering. This matrix is subjected to different conditions, like diverse air flows and oxygen concentrations. These variables affect the combustion by increasing or decreasing parameters like temperatures, velocity of the front propagation, reaction products, etc. These ranges of data may help to fight smouldering by designing special detectors, predicting the behaviour and understanding the process.

ABSTRAKT (Polish)

Celem niniejszej pracy jest uzyskać lepszej wiedzy o zachowaniu oraz charakterystyk zjawiska zwanego „tleniem" lub „żarzeniem". Jest to specyficzna forma spalania w paliwach, które znajdują się w skondensowanej fazie. Fenomen ten występuje bez płomieni, generują się niższe temperatury i rata spalania jest mniejsza niż przy normalnym spalaniu.

Nawet jeśli natura tlenia zdaje się niegroźna, stanowi to poważne zagrożenie pożarowe. Z jednej strony, procent gazów toksycznych wytworzonych przez reakcje jest bardzo wysoki, jest to częsta przyczyna ofiar w pożarach domowych. Z drugiej strony, tlenie może się rozpocząć po przez bardzo małą ilość ciepła, a następnie potrafi przejść w normalne spalanie z płomieniami, powodując w ten sposób ogromne obszary pożarów leśnych i innych katastrów.

Praca ta przedstawia informację wyciągniętą ze struktury torfu zmieszanego z piaskiem grubo ziarnistym, która jest doprowadzona do tlenia. Struktura ta została poddana rożnym warunkom, jak na przykład różne przepływy powietrza i koncentracje tlenu. Te zmienne wpływają na reakcje powodując zwiększenie lub zmniejszenie parametrów takich jak temperatura, prędkość rozprzestrzeniania się reakcji, produkty reakcji, itp. Zakresy tych danych mogą pomóc w zwalczeniu tlenia poprzez projektowanie specjalnych detektorów, przewidywania zachowania oraz zrozumienia procesu..

ABSTRACTO (Spanish)

El objetivo de esta tesis es entender mejor el comportamiento y las características de un fenómeno llamado "combustión latente". Esto es una forma específica de combustión en materiales que se encuentran en una fase muy condensada. Esta reacción se presenta sin llamas y con menores temperaturas y ratios de combustión comparando con la combustión normal donde si hay presencia de llamas.

Aunque la naturaleza de este fenómeno parezca débil, en realidad constituye un grave riesgo de incendios. Por un lado, los productos de la reacción son muy ricos en gases tóxicos, esto conduce a una elevada mortalidad en incendios residenciales. Por otro lado, la combustión latente puede iniciarse con una fuente de calor mínima, y luego desarrollarse en un verdadero incendio flameante. De esta forma se generan enormes áreas incendiadas en zonas forestales y otros desastres. Lamentablemente este tipo de combustión es frecuentemente olvidado en las comunidades de protección contra incendios.

Este trabajo presenta la información extraída de una estructura de turba mezclada con arena que combustiona latentemente. Esta matriz es sometida a diversas condiciones, como diferentes flujos de aire y concentraciones de oxigeno. Estas variables afectan la reacción haciéndole incrementar o disminuir parámetros como la temperatura, velocidad de propagación del frente de combustión, los productos de la reacción, etc. Estos rangos de datos pueden ayudar en suprimir la combustión latente a través de diseños de detectores especiales, prediciendo su comportamiento y entendiendo mejor el proceso.

List of figures.

List of tables.

Contents

1. Introduction

1.1   Literature review

Definition of Smouldering:

Smouldering is a slow, low-temperature, non-flaming combustion mode [1]. It is a self-sustaining, propagating, exothermic, surface reaction of a condensed fuel [2]. The combustion is sustained by the heat generated when the oxygen directly reacts with the surface of the material [3, 4].

The fuels that can sustain smouldering have a big characteristic thermal time and usually a tendency to char [6]. Smouldering normally happens in porous materials, where the surface area per unit volume is very large, facilitating this way the reaction. For this study, the aggregate is peat and the permeable medium is formed by grains of sand. The already reacted matrix acts as insulation, keeping the heat in the material but at the same time it allows the oxygen to reach the reaction front by convection or diffusion [1]. This characteristics make the reaction slower and with lower temperatures. Because of this, smouldering is actually an incomplete oxidation reaction. Thus, smouldering generates a high level of toxic, asphyxiant and irritating gases. For example, it favours the production of CO instead of CO_2 and HCN [3] where both spices are a very dangerous gasses for human live.

Smouldering process:

To initiate smouldering a heat source is required to increase the temperature of the material. The first thing to happen is water evaporation [6], which is an endothermic reaction that occurs at 80-100 ºC and where the emitted gases are basically water vapour [1]. After that comes the burning region; here the material starts a degradation chain reaction, where part of it is an endothermic pyrolysis. Then the oxygen reacts with the char left after the pyrolysis wave, so it is here where can be found the highest temperatures as well as the biggest mass loss. Part of this heat from the reaction is lost to the environment, and part is transferred to the material by conduction (through the matrix structure), convection (through the gasses in the pores), radiation (reradiation inside the pores and channels of the material) [1]. This process continues until the net heat from the reaction is enough to balance the necessary heat

for propagation [1]. Therefore, the two limiting factors that control the propagation of smouldering are the oxygen availability and the heat losses from the reaction front.

After the reaction front past through, what is left is a char and ash region that slowly cools down to the ambient temperature. Where the ash is the mineral content that was in the fuel and the char is the part that did not react. [1]

One of the biggest hazards that smouldering presents is the capability that it has to transform into flaming. This transition is the ignition of the gas-phase products of smouldering (pyrolysis gases, CO etc). This phenomenon can happen when some critical conditions are reached in the pores. Among others these conditions are: to be inside of the flammability limit range, enough accumulated heat released by the reaction and a good supply of oxygen to feed the fire [1].

Configurations of smouldering:

Basically, there are two ways of propagation of the smouldering front: Opposed and forward propagation.

Opposed propagation (Figure 1): In this case the reaction front propagates against the oxygen flow, so the oxygen travels along the virgin fuel until it reaches the reaction zone, then the species of the combustion and big part of heat from the reaction are transported to the char zone behind the combustion zone. Therefore, the preheating of the virgin fuel is slower as well as the propagation velocity of the front [1]. Consequently, it has a steady propagation velocity and the oxidation and pyrolysis front overlap creating only one. Transition to flaming does not happen. This configuration is more often the cause of a fire initiation, thus it has been studied more extensively.[5]
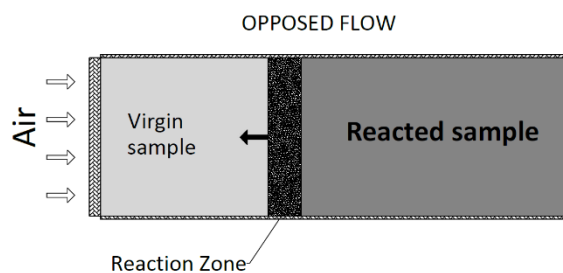
Figure 1: Schematic model of opposed flow smouldering.

Forward propagation (**Error! Reference source not found.**): The oxygen flow and the ombustion front travel in the same direction. The oxygen flows through the already reacted material attacking the reaction from behind, then the unreacted oxygen continues forward

along the virgin fuel together with the convective heat transport. With this mechanism the preheating of the fuel ahead of the reaction is much more efficient. Therefore, the propagation velocity of the front increases with higher flows and eventually transition to
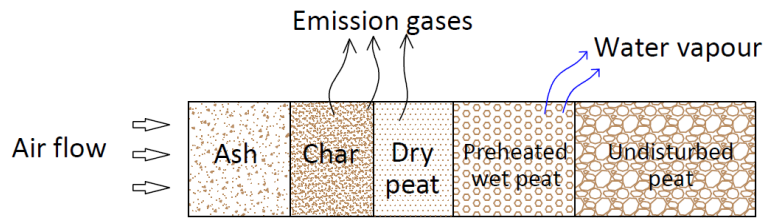
Figure 2.Schematic model of forward smouldering.

flaming can occur. So it is more dangerous fire scenario than opposed smoulder but less common [5]. According to literature, "*Forward smoulder propagation is unsteady and moves at a lower rate that appears, limited by the stoichiometry of char oxidation, for forward smoulder, two distinctive reactions were observed, a nonoxidative pyrolysis reaction and a char oxidation reaction*"[5]. In this work only this type of configuration is studied.

Representative model that describes smouldering of peat:

There are many different models in literature that try to predict smouldering behaviour, here is presented briefly a scheme developed by Guillermo Rein *et al.* which can be found in reference [6] that specifically describes smouldering of peat.

The component that makes out of peat a potential fuel for fire is the organic matter (OM). The figure bellow shows a possible distribution of the different components of peat which can vary depending on the origin of the peat sample, but typically the amount of carbon is between 30-65%. The proposed scheme is 1-step drying plus 4-step decomposition process:
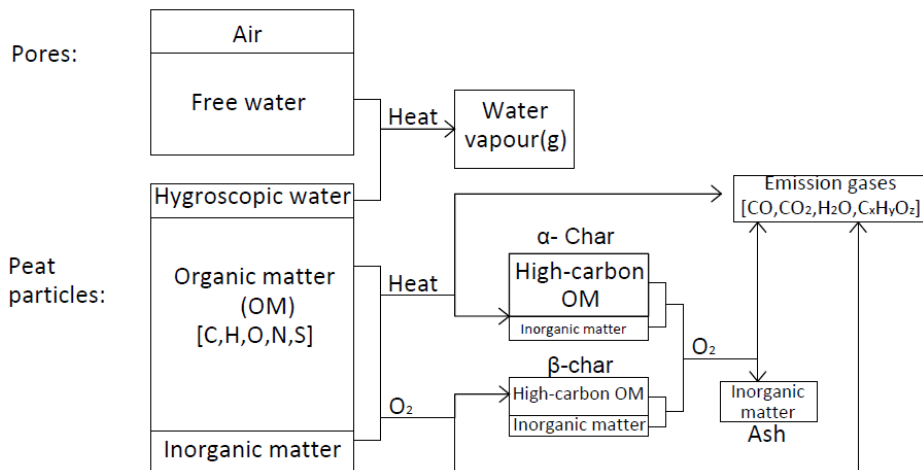
Figure 3. Composition of peat and possible decomposition paths and products.

1. *Moisture content and drying:*

Peat can hold a very big range of moisture contents (MC), the condensed-phase water can exist in two forms: hygroscopic (<10% vol.) and free (capillary and gravity, 10-40 % vol.). The water evaporates at low temperatures while the decomposition of the material is still negligible. The first water to evaporate is the free gravity water in the biggest pores, then the capillary water in the smaller ones, and finally the hygroscopic water bonded to the surface of peat particles creating a thin film of 4-5 molecules. But since peat does not ignite with higher MC than 115%, the free water content is not taken into account. The only modelled form of water is the hygroscopic one, which can exist above 100 ºC and does not flow. These gives place to the following expression:

$$Peat \cdot v_w H_2O \ \rightarrow Peat + \ v_w H_2O(g) \tag{1}$$
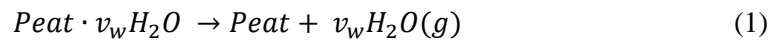
Where:

v_w – Initial MC
$Peat \cdot$ - Means that the water is bonded to the peat

So this drying step is mainly a chemical process and can be modelled with a 1-step Arrhenius expression.

2. *Peat decomposition:*

It is proposed a process of 4 steps: pyrolysis, peat oxidation, β-char oxidation and α-char oxidation. And 4 solid pseudo-species: peat, α-char, β-char and ash.

So Figure 3 is actually representing this scheme:

$$Peat \ \rightarrow \ v_{\alpha,pp}\alpha - Char + \ v_{g,pp}Gas, \quad (Peat \ Pyrol.) \tag{2}$$

$$Peat + \ v_{O_2,po}O_2 \ \rightarrow \ v_{\beta,po}\beta - Char + \ v_{g,po}Gas, \quad (Peat \ Oxid.) \tag{3}$$

$$\beta - Char + \ v_{O_2,\beta o}O_2 \ \rightarrow \ v_{a,\beta o}Ash + \ v_{g,\beta o}Gas, \quad (\beta - Char \ Oxid.) \tag{4}$$

$$\alpha - Char + \ v_{O_2,\alpha o}O_2 \ \rightarrow \ v_{a,\alpha o}Ash + \ v_{g,\alpha o}Gas, \quad (\alpha - Char \ Oxid.) \tag{5}$$
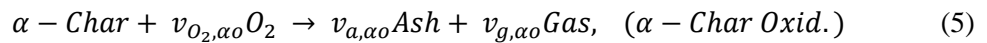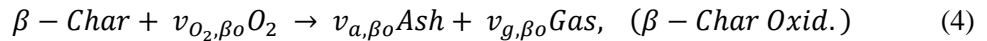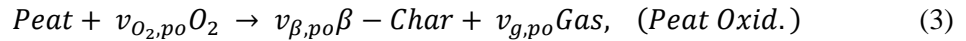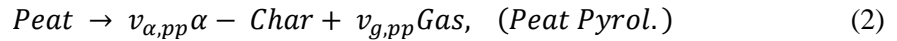
Where:

$v_{i,k}$ – Mass stoichiometric coefficient of species i=O_2,g,p,α,β,a in the reaction
k=pp,po,βo,αo

There are two different paths to follow: eq. (2)+(5) or eq. (3)+(4). Eq. (2) and (3) express the release of gaseous organic matter, so what is left behind has a lower organic content than the original peat. Both types of char have different decomposition mechanisms and reactivity, this is the reason why they are expressed separately in eq. (4) and (5)

3. *Reaction rate*

For this scheme it is used Arrhenius law, which is applicable for the reactions described in

the eq. (1)-(5):
$$\dot{w}_k\left(T, m_i, Y_{O_2}\right) = \left(m_{i,\Sigma}\right) A_k e^{-\frac{E_k}{RT}} \left(\frac{m_i}{m_{i,\Sigma}}\right)^{n_k} Y_{O_2}^{n_{O_2,k}} \tag{6}$$

Where:

A_k- Pre-exponential factor

E_k- Activation energy

n_k- Reaction order of condensed species

$n_{O_2,k}$- Reaction order of oxygen in the reaction k

$m_{i,\Sigma}$ - cumulative mass, defined as $m_{i,\Sigma} = m_{i,0} + \int_0^t \dot{w}_{f_l} dt$

4. *Mass evolution in thermogravimetric experiment:*

$$\dot{m}_w = -\dot{\omega}_{dr}$$
$$\dot{m}_p = -\dot{\omega}_{pp} - \dot{\omega}_{po}$$
$$\dot{m}_\beta = -\upsilon_{\beta,po}\dot{\omega}_{po} - \dot{\omega}_{\beta o} \tag{7}$$
$$\dot{m}_\alpha = -\upsilon_{\alpha,pp}\dot{\omega}_{pp} - \dot{\omega}_{\alpha o}$$
$$\dot{m}_a = -\upsilon_{a,\beta o}\dot{\omega}_{\beta o} - \upsilon_{a,\alpha o}\dot{\omega}_{\alpha o}$$

Therefore, the total mass-loss rate of a sample is:

$$\dot{m} = \dot{m}_w + \dot{m}_p + \dot{m}_\beta + \dot{m}_\alpha + \dot{m}_a = -\dot{\omega}_{dr} + \left(\upsilon_{\alpha,pp} - 1\right)\dot{\omega}_{pp} + \left(\upsilon_{\beta,po} - 1\right)\dot{\omega}_{po} +$$
$$\left(\upsilon_{a,\beta o} - 1\right)\dot{\omega}_{\beta o} + \left(\upsilon_{a,\alpha o} - 1\right)\dot{\omega}_{\alpha o} \tag{8}$$

To sum up; this scheme is a system of equations with 18 unknowns. To solve this, it is

needed a multi-dimensional optimization algorithm like the Genetic Algorithm (GA) which

has been successfully applied. The assumptions and techniques used to solve the GA are

explained in reference [6].

Consequences of smouldering:

Even though this topic is not widely studied, it represents a hazard in many scientific and

industrial areas: Due to the high concentration of toxic gasses in the species of the reaction

and the capability of ignition from little heat sources, smouldering is the leading cause of

deaths in residential fires [1]. Moreover in the industries (e.g. aerospace industry) it is an

increasing risk, because it use to appear in hidden places that normally cannot be detected or

extinguished. Also the ecologist are concerned, because smouldering wildfires destroy huge

amounts of biomass causing big damage to the soil (For example: Smouldering is capable to

penetrate deep into the ground by propagating through the roots of the trees and burning

everything on its way, but also making it very difficult to extinguish, since the combustion

can be several meters below the ground level). This type of fires represent a significant

contribution to the atmosphere pollution. [1]

Nonetheless, there can be also benefits from smouldering, as some of the new technologies are based on the straight application of it. Among other, remediation of contaminated soils, production of biochar for long terms storage, etc. [1]

1.2 Objectives

Peatlands are an accumulation of partially decomposed flora and they are the largest and most frequent ecosystems affected by smouldering fires. They are the biggest reserves of carbon as well as represent an important element in the global wildlife chain. Peat can form layers of carbon older than 10 thousand years and dozens of meters depth. [7] Thus, once this huge accumulation of fuel is ignited it can burn for years representing the largest fires on Earth as well as big contributions of greenhouse gases [6]

So the objective of this study is to contribute in preventing this disasters by doing micro-scale experiments. As the combustion process in the smouldering phenomenon is a complicated chain of reactions, it is difficult to predict what is exactly happening in the atomic level, this is the reason why another way to study and understand smouldering is to investigate more measurable characteristics of it.

The experiments that are performed for this work, consist of forward propagation smouldering, where the sample is peat mixed with sand. The characteristics of the samples remain equal for all the tests. What will change is the air velocity through the sample for one set of experiments, and for other set of experiments, the oxygen concentration keeping the total flow constant.

What is directly measured are the temperatures in function of time which are registered thanks to the data logger. Other parameters are derived from these data. Like velocity of propagation of the reaction front, reaction front thickness, etc.

Thanks to this type of experiments more information will be available about the range of temperatures, velocities and other characteristics that smouldering can present.

To understand better the mechanism of this process parameters like thickness of the combustion front, the concentration of the oxygen depleted are analysed giving some information back that could fill the gaps of the actual knowledge.

Also this experiments could contribute to a better understanding of the behaviour of smouldering in natural contexts. For example where different wind speeds blow through peatlands, so it could help in the prediction of the time on which the smouldering front can reach certain point and prevent the fire to sprea

2 Methodology

This work summarizes three different types of experiments that are presented in this chapter.

2.1 Experiments type-1.

2.1.1 Objectives.

Check how different air velocities, that course through the sand and peat matrix, affect the temperatures and the velocities of the propagation front.

2.1.2 Description of the experimental setup.

The same sample type in the apparatus of Figure 4 was submitted to the following air velocities:

Air velocity through the matrix [cm/s]									
0.41	0.83	1.66	2.82	4.06	5.80	7.56	9.95	10.78	13.26

Table 1 Values of the inlet air velocities for experiments type-1

For these experiments it is used a mixture of sand-peat, where the relation is: 4% peat and 96% sand in mass, the total mixture weight is 4 kg. This relation was chosen because with lower amounts of peat the combustion has frequent tendency to extinguish and on the other hand, bigger concentrations of peat gave place to flaming, especially closer to the surface zone where more oxygen is available (phenomenon that would definitely effect the results with much higher temperatures than expected, that is the reason why it should be avoided) In order to avoid moisture as another variable. The peat is dried for at list 24h in the oven at 80 °C.

The apparatus in which the mixture is burned is called "STAR" (Figure 4), it consists of a metallic cylinder open in the top, with insulation around it, a heating wire at the bottom for starting ignition and an air diffuser also at the bottom of the cylinder.

Figure 4. Apparatus setup for experiments type-1.
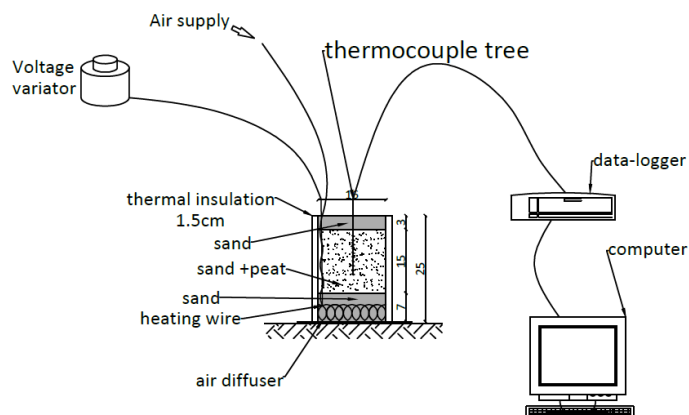
The first 7 cm at the bottom of the cylinder are covered with sand (so it covers the heating wire and air diffuser). This way the boundary conditions next to the wire are softer. Then the second and thickest layer is the mixture sand-peat (where the smouldering combustion is taking place), and the third and last layer is of about 3 cm of sand again (it is to avoid bubbling of sand-peat mixture when the smouldering front is close to the surface, as well as to avoid flaming and other boundary conditions that may influence the smoulder occurring inside the cylinder).

A thermocouple tree (with ten thermocouples separated every 1cm) is placed vertically in the middle of the cylinder, where the first thermocouple is ~3 cm above the 1st layer of sand that covers the heater.

Once everything is settled a voltage of 190V is applied to the wire. When the first thermocouple registers a temperature of 200 °C the air starts to flow through the diffuser. The heater is turned off once the combustion is self-sustainable, normally this stage is considered when at least one thermocouple registers a temperature pic of around 500°C.

2.1.3 Analysis method.

In this section it is explained the process that is used to analyse the data recorded in the data-logger:

Graph 1 is an exemplar test and it represents straight forward the temperatures that are registered by the thermocouples every 2 seconds:
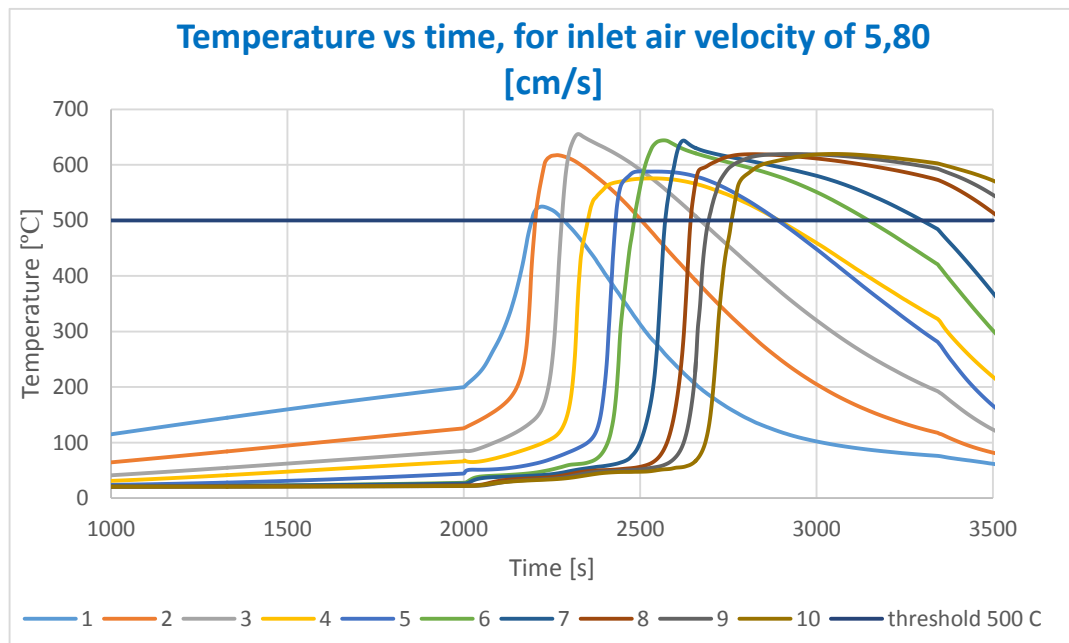
Graph 1. Experiment type-1, results from the test with inlet air velocity of 5,80 [cm/s]

Each curve from Graph 1 represents the temperature as a function of time for a given thermocouple (for given position). Where the curve number 1 is the closest thermocouple to the bottom of the cylinder and the curve number 10 is the farthest one.

2.1.3.1   *Temperature analysis:*

One of the parameters to be analysed is the temperature of the combustion. As it can be observed in Graph 1 each thermocouple registers different maximums for the temperature. So, four different procedures are followed in order to define the combustion temperature for a certain air velocity:

1. Average of the maximum value of all the thermocouples.
2. Average of the maximum value of all the thermocouples discarding the three lowest maximums.
3. Average of the maximum value of the last five thermocouples (steady state).
4. The highest recorded temperature during the test.

2.1.3.2   *Smouldering propagation velocity:*

The other factor that is studied is the velocity at which the reaction propagates through the matrix. In an ideal situation, this should be checked by calculating the time between two neighbouring thermocouples when they reach their maximum temperatures. The velocity in that interval would be the division of the distance between that thermocouples by the previous defined time. But these pics are not regular enough, so this method would not work. Instead of that, a threshold value is defined close to the maximum values (In the exemplar test the value is 500 ℃). Therefore instead of looking for the time between the maximum points, it will be the time between the points at 500 ℃.

To automatize the calculations, Graph 2 is generated in Excel:

Graph 2. Experiment type-1, velocity of the thermal wave of 500ºC, for the test with inlet air velocity of 4,06 [cm/s]
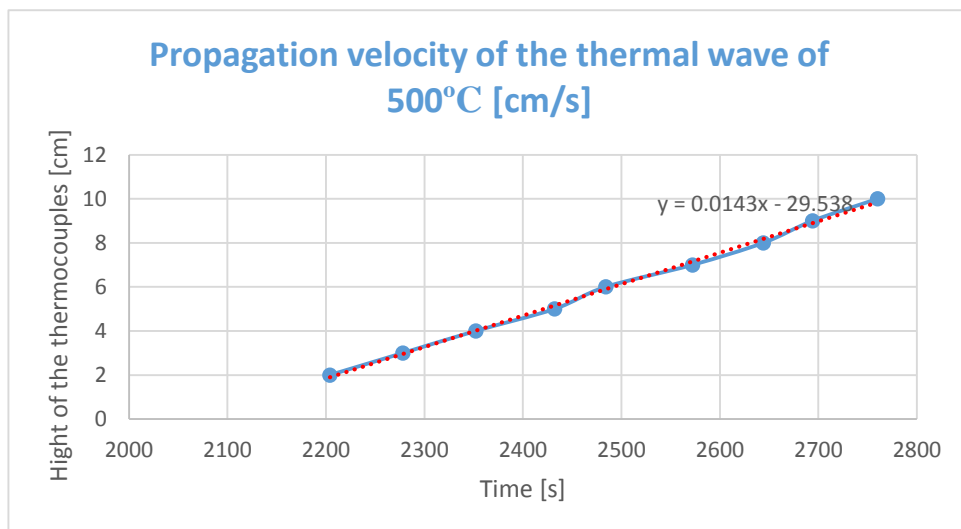
The blue curve represents at which time the value of 500 ºC is reached by a given thermocouple. The red line is a linear approximation of the curve, assuming that the velocity is constant along the height of the cylinder. The slope of the linear approximation is the velocity of thermal wave, in this case it would be 0.0143 cm/s.

The same procedure is used for all the tests so the results can be comparable. Along all this documents it is assumed that the velocity of the thermal wave is equivalent to the propagation velocity of the smouldering zone.

2.2   Experiments type-2.

2.2.1   Objectives.

Check how different oxygen concentration affect the reaction temperatures, the velocity of the propagation front, the temperature profiles and the thickness of the combustion front.

2.2.2   Description of the experimental setup.

7 kg of the same mixture as before is submitted to different gas mixtures with constant inlet gas velocity of 2.16 cm/s. The oxygen concentration is controlled by adding an inert gas to the gas mixture, in this case nitrogen.

Oxygen flux [g/s·m^2]							
6.50(air)	5.85	5.20	4.55	3.90	3.25	2.60	1.95
Translated into percentage of N$_2$ mixed with air [N$_2$ %]							
0	10	20	30	40	50	60	70

Table 2. Oxygen concentrations applied in the inlet gas for the tests in experiments type-2

For this type of experiments it is designed a new apparatus (Figure 5Figure 5). It consists basically of a longer cylinder with a smaller diameter. By this change it is reached a bigger length where the boundary conditions from the top and the bottom can be neglected, as well as the problem becomes more one-dimensional so the reaction moves in one upward direction as well as the air distribution is more uniform along the cross section.
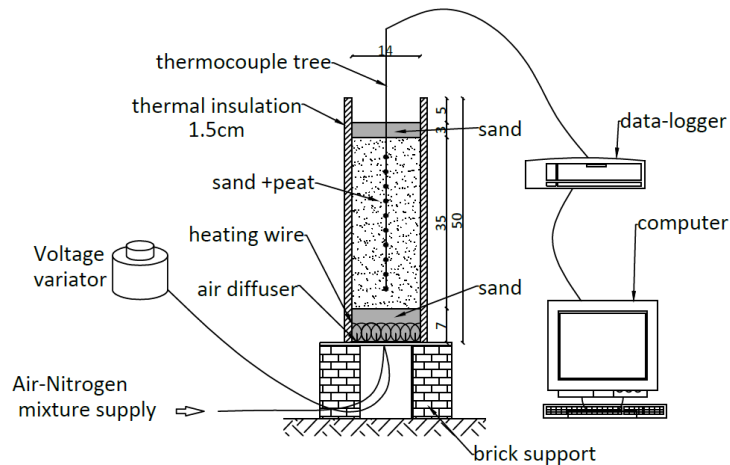
Figure 5. Apparatus setup for experiments type-2

The thermocouple tree is adjusted, so the thermocouples are now every 3cm.

Since the amount of energy given into the system in order to start the ignition can vary the results, to be more precise in this case, the heater will be working with a power of 190V during 40 min. After this time the gas mixture starts to flow and the heater is turned off. For all the experiments it is applied the same procedure to be sure that the initial energy in the system is equal for all the tests.

2.2.3   Analysis method.

The temperature of the reaction and the velocity of the propagation front are measured equally as in the experiments "type 1".

2.2.3.1   *Smouldering propagation velocity:*

There is only one small difference when measuring the spread velocity: As the column is much longer, the compaction of the matrix is not negligible any more. This happens because when the peat is burned, it leaves free spaces behind, making the all structure weaker. And since now there is more weight on the structure, the matrix will start to compact gradually after some point.

So, in the first overview of the experiment, it looks like the reaction slows down. The reason for that, is that there is a bit of an effect where the reaction, instead of moving through the fuel, the fuel "comes to the reaction". In order to take this into account, the centimetres of compaction are measured and then they are added between the distances in the last thermocouples.

The next figure shows the error that the compaction may cause in an exemplar test:

Velocity of the propagation front [cm/s] for a oxygen flux of 3.90 [g/s·m²]

$y = 0.0054x - 21.514$

Hight of the thermocouples [cm]

Time [s]

— distance not corected   — corected values of the distance

······· Linear (corected values of the distance)
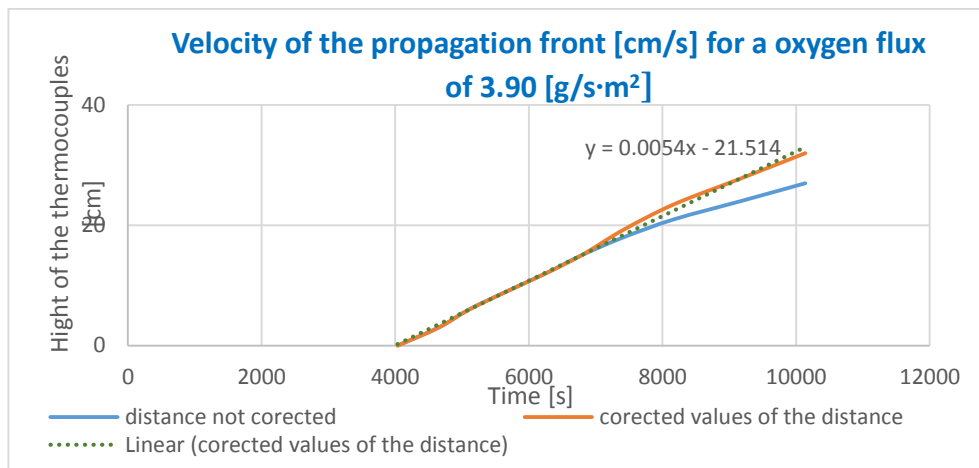
Graph 3. Effect of the matrix compaction phenomenon

2.2.3.2   *Analysis of the reaction front thickness:*

Other objective of this projects is to measure the thickness of the reaction front or to establish if this thickness reaches steady state. To solve this problem there were tried two approaches:

2.2.3.3   *Approach 1:*

Establishing the thickness as the space between a chosen threshold temperature value. The graph below shows the speed of the thermal wave propagating along the sample. There were chosen two threshold values: 400 ºC and 500 ºC.

Velocity of the thermal wave, oxygen flux 6.50 [g/s·m²]

Hight of the thermocouples [cm]

Time [s]

— 400 C isotherm heating wave

— 400 C isotherm cooling wave

— 500 C isotherm heating wave

— 500 C isotherm cooling wave
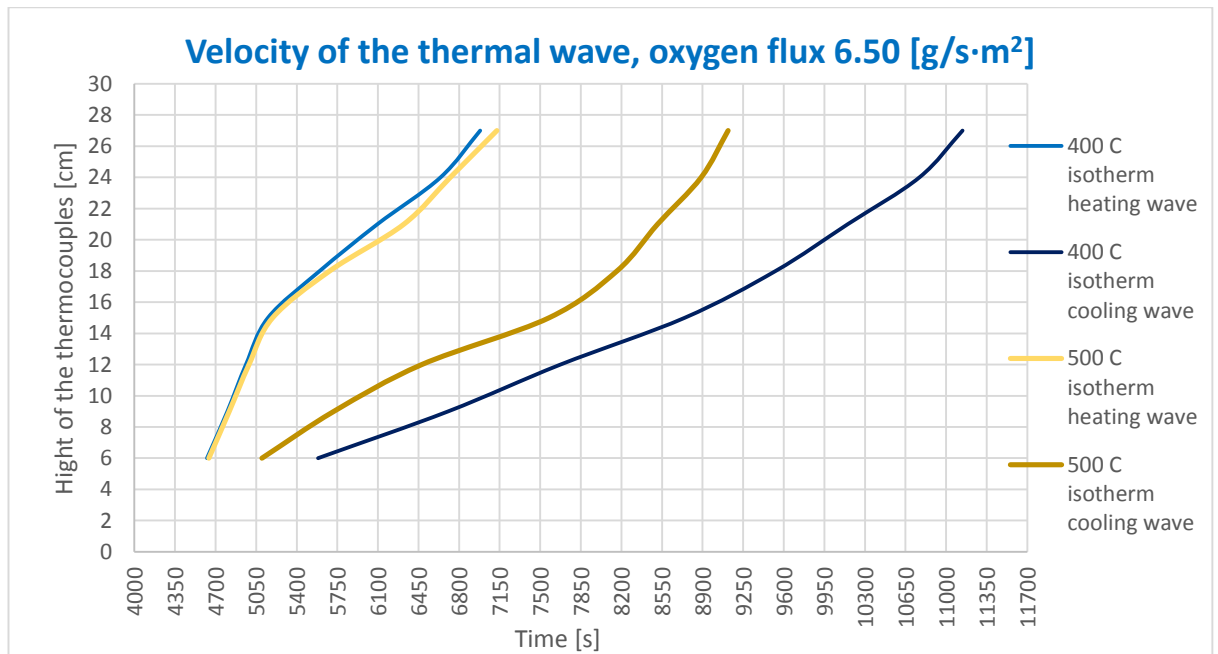
Graph 4. Position of the heating and cooling thermal wave. Two thermal waves are analysed: 400ºC and 500ºC

12

The curve "400 ºC isotherm heating wave" means at what time which thermocouple reaches the value of 400 ºC, in the forward preheating process of the sample. Vice versa, the curve "400 ºC isotherm cooling wave" means at what time which thermocouple reaches the value of 400 ºC, in the cooling process. Exactly the same explanation answers the other curves, just with 500 ºC as threshold.

By using this scheme, it is impossible to define the thickness of the reaction, as it depends of the chosen threshold value. The parameter that could be checked is if this thickness reaches steady state.

Thus, it is subtracted from the isotherm that represents the heating wave the corresponding isotherm that characterise the cooling wave. This way it is obtained the thickness of the sample, which is at the temperature of 400 ºC and above, or 500 ºC and above.

This subtraction of the two curves is represented in Graph 5:

Thickness of the sample between chosen thresholds temperatures, oxygen flux 6.50 [g/s·m²]
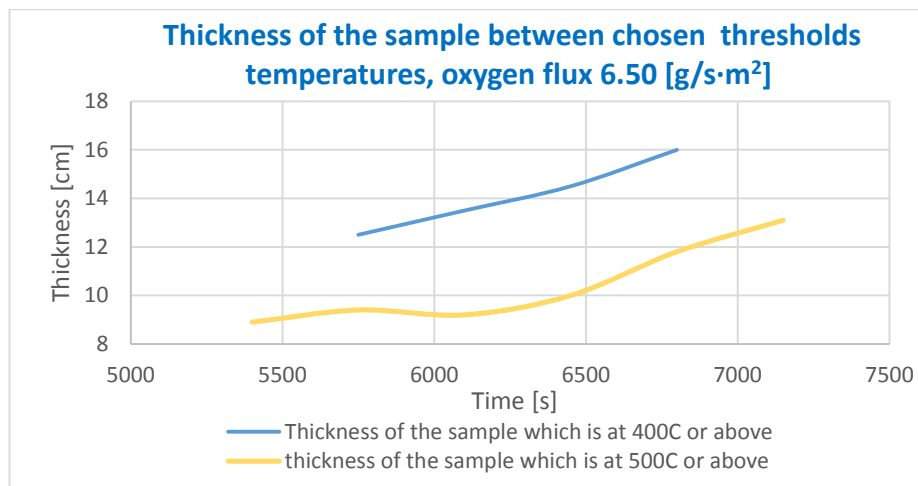
Graph 5. Thickness of the sample that has a greater temperature than the threshold values of 400ºC and 500ºC

Independently of the chosen curve, it can be seen that the thickness is increasing by time, this could mean two things:

1. The thickness of the reaction front does not reach a steady state conditions, as it is getting wider by time.

2. The reaction front reaches steady state. But in the heat balance, the heat losses are smaller than the heat production from the reaction. Therefore the tube should be much longer to reach energy balance. In this case, the cooling air from the bottom is less and less effective since it has to travel through a longer and longer heated matrix. That way the speed of the cooling wave decreases, increasing the thickness of the sample at a threshold temperature value or above.

Consequently, this methodology is interrupted because it is not really providing a solution for the problem.

2.2.3.4   Approach 2:

Establishing the thickness as the range, in which the *temperature-profile curve* appears in a convex form.

Therefore, the temperature-profiles curve over height, as it is shown in Graph 6, is the tool that provides this information.
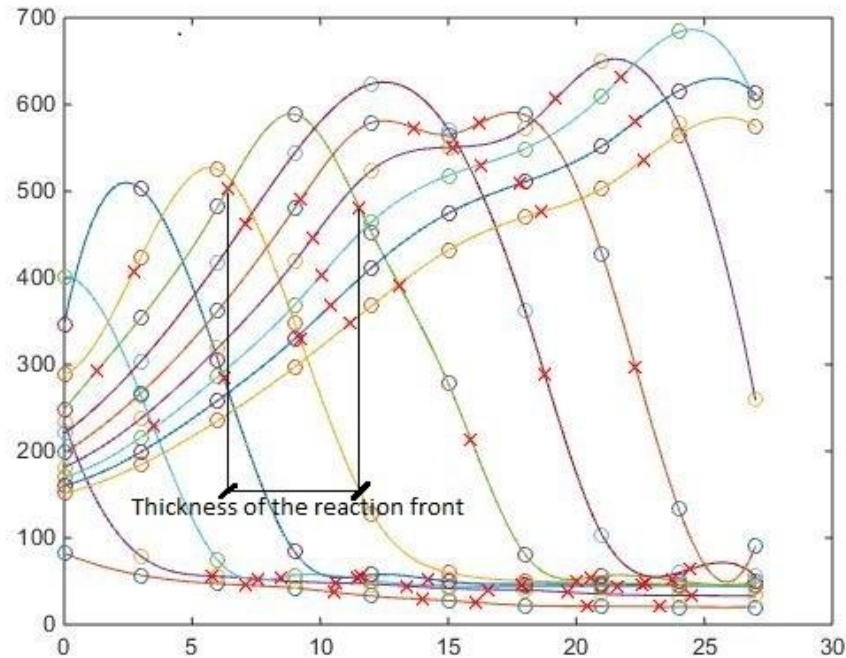
Graph 6. Exemplar temperature-profile curve for experiments type-2

Each curve represents the temperature profile for a given time, where the first curve signifies the situation when the heater is turned off, the next one is 5 minutes after and so on.

On the X-axis is plotted the height of the cylinder and on the Y axis the temperatures. This figure is a result from the software MATLAB where the circles are the specific values from the experiments and the crosses are the inflection point of the curves. To define the thickness of the reaction front first has to be defined where the curve is convex, and then calculate the interval where this convexity appears. If the curve is convex in more than one interval, only the interval with the highest temperatures should be taken into account, because it is there that the reaction is located.

Methodology used in MATLAB:

1. Introduce a matrix with the data from a test.
2. Interpolation between the points: every interval is defined with a polynomial equation of grade 4, the origin of each equation is located at the first point of the interval.

3. MATLAB generates a matrix with the coefficients of the polynomials, where the columns are the coefficients corresponding to the variable x^3, x^2,x,n.

4. Finding the inflection point $\Rightarrow f''(x) = 0$. The following command to the matrix with the polynomial coefficients is applied: $x = \frac{-2_{i,2}}{6_{i,1}}$

5. Add to the previous result the distance to the original origin, locate this results in the plot with crosses.

The weak point of this method is that the output depends a lot of the interpolation that is done between the points, a different way of interpolating may change the concavity of the curve. Therefore, the inflection points would be placed in other positions and consequently the sought thickness would change.

In order to get a more accurate temperature profile curve and diminish the influence of the interpolation between points a new thermocouple tree is built with 24 thermocouples. This was not done before because with a big number of thermocouples the overall diameter of the thermocouple tree increases, and this may provoke a "chimney effect". So the gasses instead of going through the matrix, go only through the channel in the centre made by the thermocouples.

Thus, the repeats of the test with 10, 20 and 30% of Nitrogen are performed with the new thermocouple tree in order to define more accurately the front thickness.

Graph 7 shows the temperature-profile curve recorded with the new thermocouple-tree:
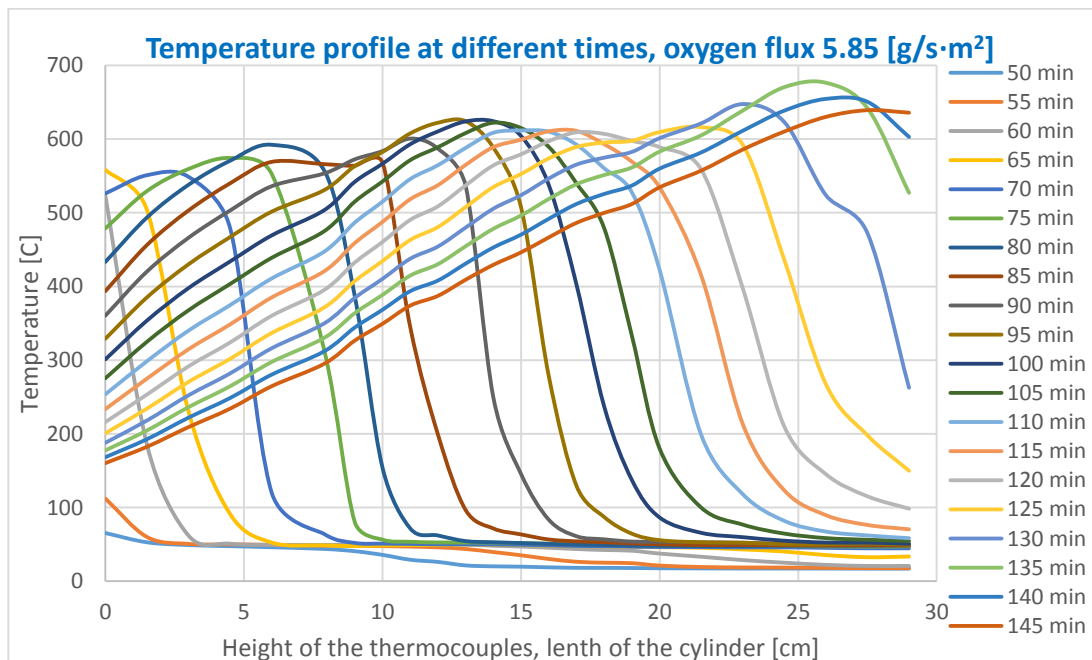
Graph 7. Exemplar temperature-profile curve for experiments type-2, performed with 24 thermocouples.

Now, a new problem appears. Namely, since the temperatures are measured in 24 points the curves do not look smooth any more, it can be appreciated the presence of many fluctuations. This irregularities trigger much more inflection points than expected.

One way to avoid this problem would be that instead of doing an interpolation from point to point, it would be better to do an approximation curve that will go close to each points within an established margin error. So in future work a new MATLAB code should be developed to get more realistic temperature-profile curves.

For this work the analysis of the thickness of the reaction front is done with the original thermocouple tree.

2.3   Experiments type-3.

2.3.1   Objectives.

Check how different oxygen concentrations in the inlet influence the oxygen concentration in the outlet and make an estimation of the consumed oxygen.

2.3.2   Description of the experimental setup.
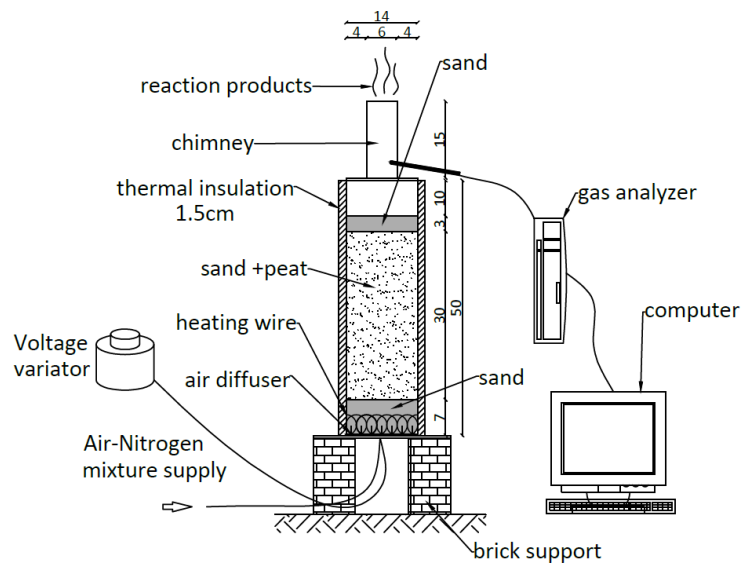
Figure 6. Apparatus setup for experiments type-3

These experiments are under the same conditions as experiments type-2, but instead of measuring the temperatures it is measured the oxygen in the outlet (the oxygen that did not take part in the reaction). For the gas analysis, a cover with a chimney is designed. The cover is sealed to the cylinder with aluminium type before every experiment to prevent leaks. Then a tube is connected to the chimney which sucks the gases to the gas analyser.

Since the species are not diluted with air, the concentrations of CO and CO_2 are so high that they surpass the upper limit of the gas analyser, this is the reason why only the concentration of the oxygen is analysed in this work. Also all the filters of the gas analyser should renewed after every test, because the condensation and the amount of ash in the species is so high that they completely fill the filters.

2.4 Recognised limitations and errors of the experiments.

1. Since smouldering is happening in a metallic cylinder, even though there is insulation around it, there will be always some heat losses through the walls of the cylinder which are very difficult to quantify, triggering lower temperatures.

2. As it was explained before the sand is mixed with peat. Even though, the final mixture is not homogenous of sand and peat powder, there are always bigger kernels of peat remaining. Depending on the position of these kernels in the matrix (e.g. touching directly the thermocouples) they can influence the temperature registered in a given thermocouple.

3. Other limitation or source of error, is that these thermocouples are type K, so the recorded temperatures are not punctual, because the unprotected surface of the thermocouple influence the logged temperature, so actually the thermocouples should be placed parallel to the temperature gradient lines. But this is impossible in this setup, the only way to place the thermocouples into the cylinder is vertically through the top, so in this case the unprotected area of the thermocouple is lying in a region with a temperature gradient.

4. In the experiments type-1, the air that flows through the diffuser is taken straight from the compressor, which may change its pressure during the experiment diminishing the flow to the experiment. Even if all the tests were supervised and this pressure drops were adjusted with a manual flowmeter, the flow was not perfectly constant by time. This problem was not present any more with the other types of experiments, because the gas flow was controlled by automatized mass flow meters

3 Results and discussion

In this section it is presented and explained the results from the experiments, especially it is focused to describe the trends that smouldering presents for the different setups.

3.1 Experiments type-1.

3.1.1 Progress of the tests.

The graph below is a representative output from the data-logger in this type of experiments, all the other test results are attached in appendix A.
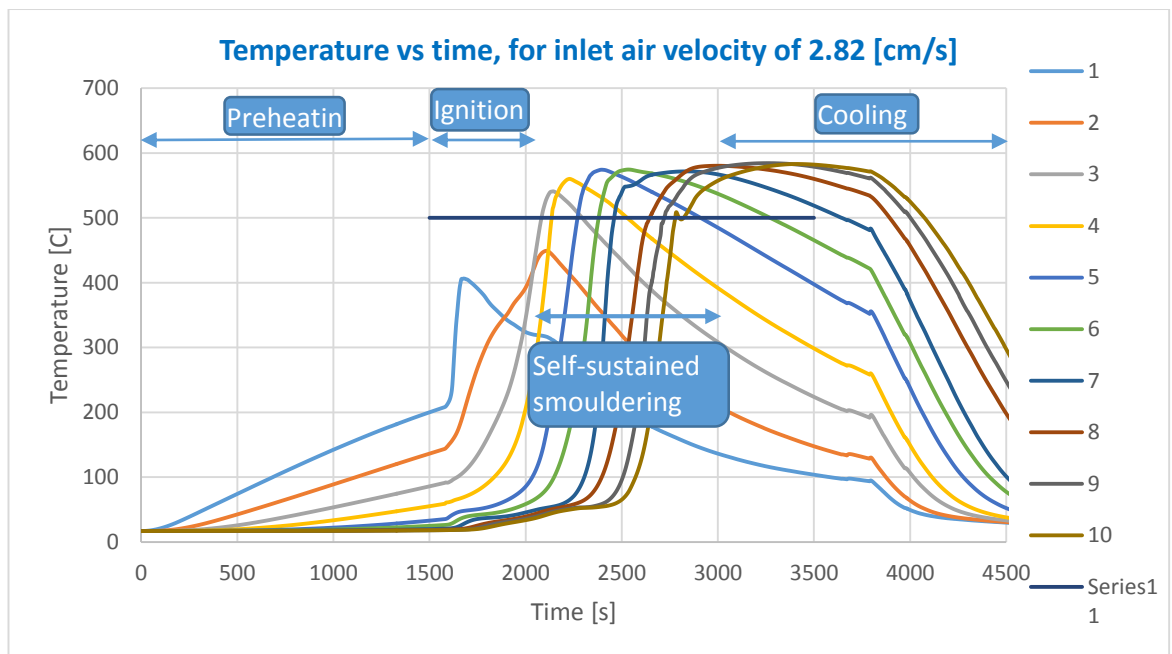
Graph 8. Exemplar output for the experiments type-1

As explained in the methodology section, a given curve represents the temperature as a function of time for a given thermocouple (for given position). First the sample is preheated, as it can be observed, on the right hand side there is a linear growth of temperature since the heat given into the system is through the heating wire, which works at a constant power. So the points closer to the wire have higher temperatures that the farther ones.

At the moment $\sim 1600s$ there is a big change of slope, this is because in this moment air starts to flow through the matrix and it ignites the peat. Since the reaction started, the jump in temperatures is very big. Now the source of heat for the next layers of sand-peat mixture is

the reaction itself. Then, the mechanism is that the products of the reaction heat up the next layers. The forces that drive the hot gasses to move upwards are specially the momentum force due to the diffuser at the bottom that is constantly blowing air and the buoyancy force because the reaction gasses are much hotter than other gasses in the matrix. Once the first layer finished combustion because there is no more char to react with, the oxygen starts to react with peat in the next layer, which is warm enough because it was preheated with the hot gases from the reaction below it before. And this process continues until the reaction reaches the last layer in which there is only sand causing the end of the propagation.

Each thermocouple has a maximum point, with the highest temperature, where the reaction is in its most efficient stage, and after it there is a short period of time where the reaction losses its efficiency and finally dies in that specific point. Then the cooling down process begins. The first thermocouples cool down much faster that is why the slope of the curves on left hand side of the maximum points are much steeper than the slopes of the last thermocouples. This is because the first thermocouples are closer to the diffuser so the air flowing in that position is still cold. But then the air has to continue flowing through all the height of the cylinder and it warms by convection because the sand (which has a very high thermal capacity) remains very hot after the reaction. That is the reason that when the air arrives to the last thermocouples is so hot that the cooling down is much less efficient.

3.1.2 Temperature analysis.

After repeating the experiments several times with different airflows Graph 9 is plotted:
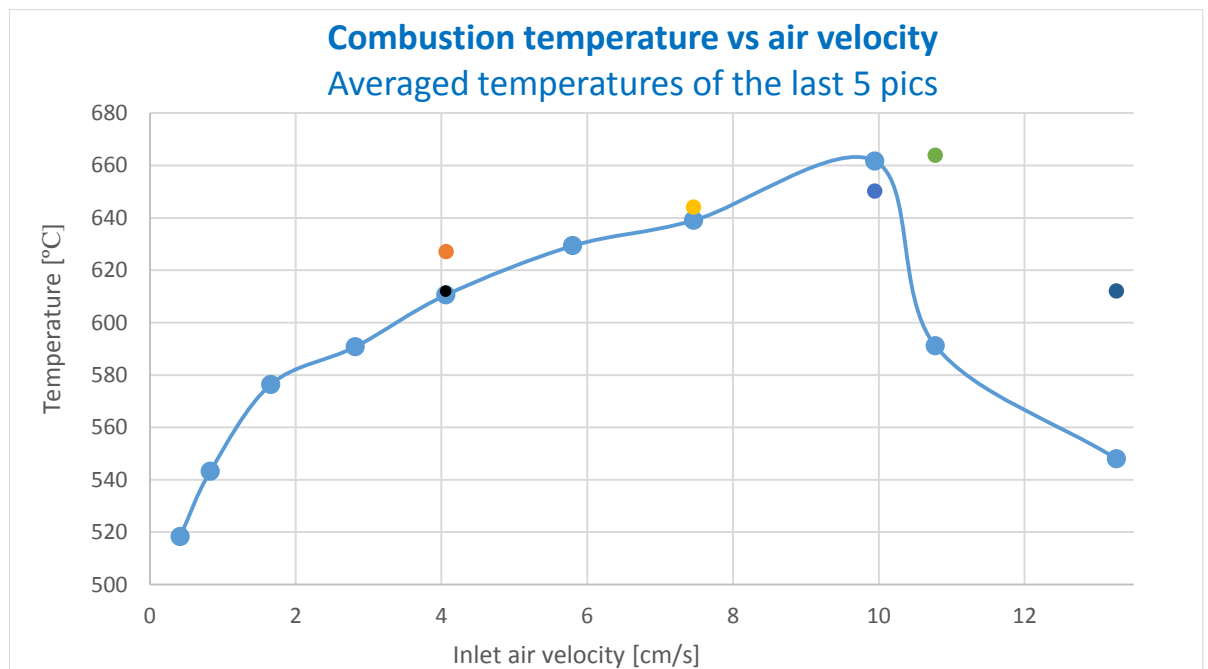
Graph 9. Trend of smouldering temperatures for different inlet air velocities. Information extracted from tests attached in appendix A.

Graph 9 shows how smouldering combustion increases its temperature when air flow increases. This trend can be appreciated with many ways of averaging, and additionally the colourful dots prove the repeatability of the experiments. This increase of temperature happens until certain flow, then the temperatures start to decrease. This is due to the fact that the reaction only uses part of the oxygen in the air, the unreacted oxygen and the nitrogen that do not play a role in the reaction are actually cooling down the system. Consequently after some point the amount of this gases is so big that the cooling effect is leading above the heating from the reaction.

This observation matches with the literature. Even though, usually it is not mentioned the limiting condition of the cooling effect.

It is also important to mention that the interpretation of the results plays a big role. The following graph summarizes some of the possible ways for defining the smouldering temperature. Thus, it is necessary to analyse each test individually and to know which data should be discarded and which can be kept for further analysis.
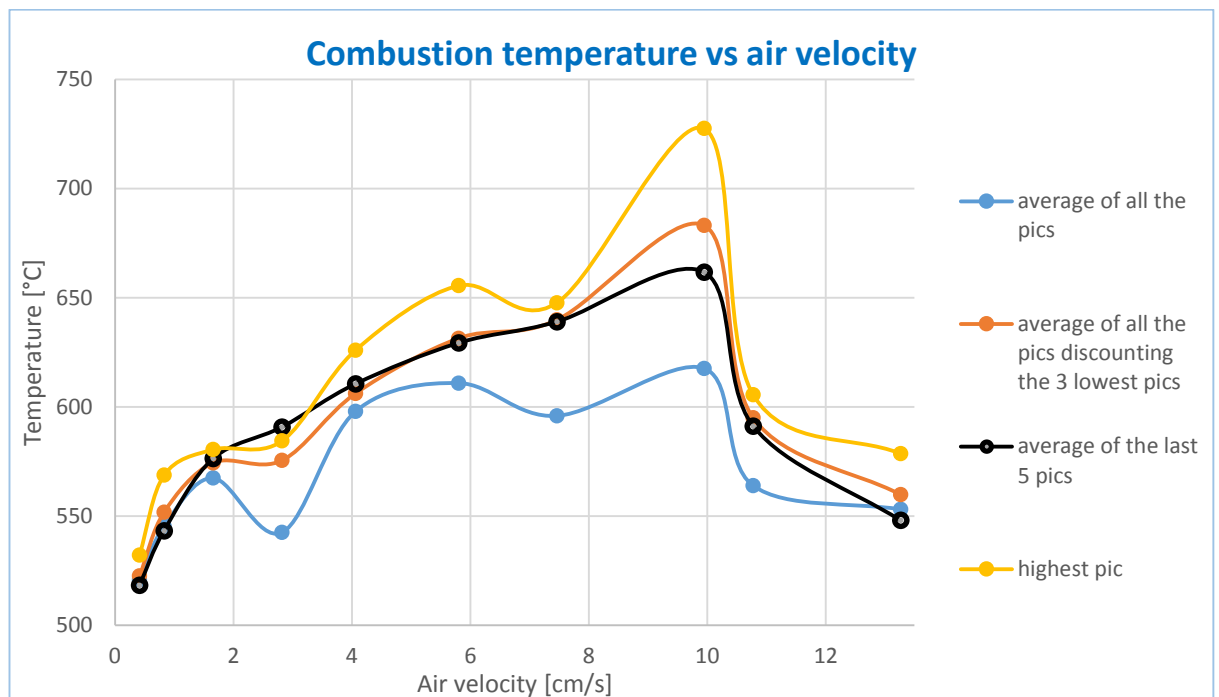
Graph 10.Trend of the smouldering temperature for different inlet air velocities and different ways of averaging the temperatures. Information extracted from the tests attached in appendix A

The reason why Graph 9 is considered the most reliable, is because it focus more in the part of the experiment which is farther from the ignition moment. The thermocouples closer to the bottom often show the beginning of smouldering, resulting with lower temperatures and changing the total average.

The explanation of the previous behaviour, where the temperatures first increase and then decrease with bigger inlet air velocities, can be summarized by the following figure:
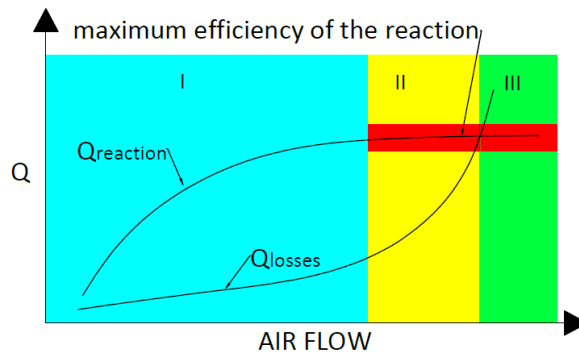

Figure 7. Schematic trend of the energy produced by the reaction vs the energy lost to the environment for increasing inlet air flow.

The increase and decrease of the temperatures of the studied system depends of the heat generated by the reaction and the heat losses from the reaction zone to the environment.

Individual evaluation of each curve:

- The heat of the reaction increases with the flow, because with more air flow, also comes more oxygen flow. With more oxygen, the combustion is more efficient, because more peat can burn at the same time. Since there is more oxygen available, the ratio CO_2/CO will increase, meaning that the reaction is closer to the complete combustion and producing more heat. Other aspect is that the preheating of the material is more efficient, so the oxidizer is reacting with a hotter reactant generating higher temperatures.

- The heat losses also increase because of two reasons:
    1. By Conduction: Since there is a temperature difference between the reaction zone and the environment, the losses by conduction increase when the temperatures increase.
    2. By convection: On one hand there are heat losses by natural convection from the walls of the cylinder to the ambient air. On the other hand, there are heat losses by forced convection from the sample to the forced flow through the matrix.

In section I of Figure 7, the arise of heat generated by the reaction thanks to the increasing flow is bigger than the heat losses. Therefore the temperatures increase.

In section II, the reaction reached its maximum efficiency, it means that all the peat is burning at its maximum rate and more oxygen provided is not going to invigorate the combustion. Therefore, while the peat burns at its maximum rate, the heat losses continue

increasing due to the bigger air velocities through the pores. This situation ends up with the decrease of temperatures.

Finally in section III, the flow is so high that the heat losses overcome the heat production, and the reactions dies.

For this problem it is possible to do a parallelism to compartment fires, and whether they are in fuel-controlled regime (section II) or in ventilation-controlled regime (section I)

In the fuel controlled regime, the excess air entering the compartment (in this case: the cylinder) moderates the temperature. The limit between the regimes depends in the relation $\dot{m}_{air}/\dot{m}$ [8] :

$$\frac{\dot{m}_{air}}{\dot{m}} < r\frac{kg}{s} \implies ventilation - contolled \qquad (9)$$

$$\frac{\dot{m}_{air}}{\dot{m}} > r\frac{kg}{s} \implies fuel - controlled \qquad (10)$$

Where:

$\dot{m}_{air} - rate\ of\ inflow\ of\ air$
$\dot{m} - burning\ rate\ of\ the\ fuel$
$r - stochiometric\ air/fuel\ ratio$

Following this parallelism, the test for compartment fires end up with the following plot which presents a similar behaviour as for the smouldering case.
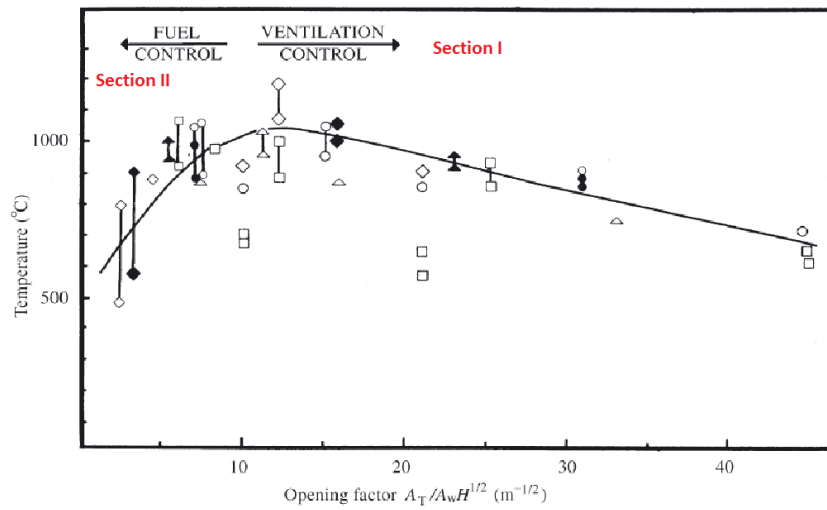

*Figure 8. Experimental results from compartment fires*

Where

A_T - Internal surface area of walls and ceiling, excluding ventilation openings [m^2]
A_w – Area of ventilation opening [m^2]
H – Height of ventilation opening [m]

### 3.1.3   Analysis of the propagation velocity of the smouldering front.

This section discusses how velocities can vary depending on the flow under which smouldering is submitted. The graph below shows the height of the thermal wave of 500 ℃
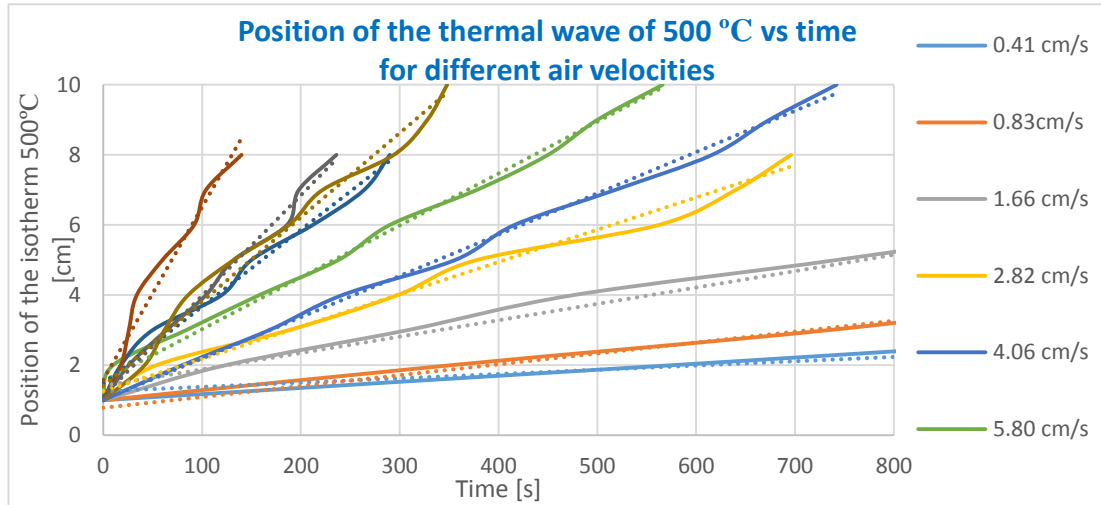
by time, being then the slope of each curve, the velocity of propagation. It can be already appreciated that the slopes become steeper with higher flows.

Graph 11. Compilation of all the tests of experiments type-1. Influence of the inlet air velocity to the speed of propagation.

After calculating all the slopes of the linear approximations of the curves from Graph 11, it can be appreciated an increasing trend of the smouldering velocity for higher inlet air velocities as presented in Graph 12. The trend cam be approximated with an exponential function. There is a strict relation between the temperatures and the velocities of the
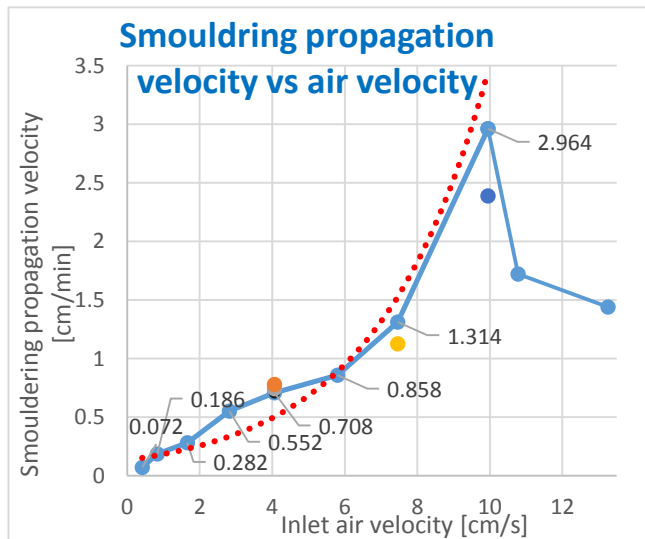
smouldering front. It can be observed clearly, that the temperatures increase when the velocity increase, and that both parameters start to decrease under the same condition.

Additionally this results can be compared to previous tests (Figure 10**Error! Reference source not found.**) where it is shown the dependence of the rate of spread of smoulder along a bed of cellulose powder on the free-stream air velocity. Here it could be deduced that the velocity increases exponentially with the air flow independently

Graph 12. Velocity of the smouldering front for different inlet air velocities. Experiments type-1.

of the material. The difference between both experiments is that Figure 9 does not present a decrease with higher flows, because that material was more likely to present transition to flaming.
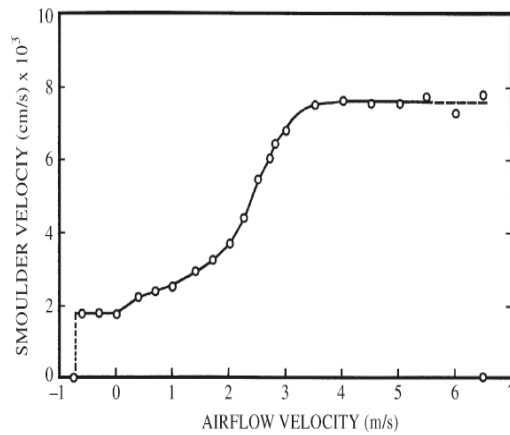

Figure 9 Experimental results of Sato and Sega 1988

However, the previous deduction does not match with the results obtained by Torero et al. [5], who concluded that the increase is linear as shown in Figure 10. This might be because the studied range of inlet gas velocities is just covering relatively low velocities. So, the obtained curved by Torero, is representing the beginning of the exponential curve that was found in the tests performed for this work, where it can still be interpreted as a linear increase.
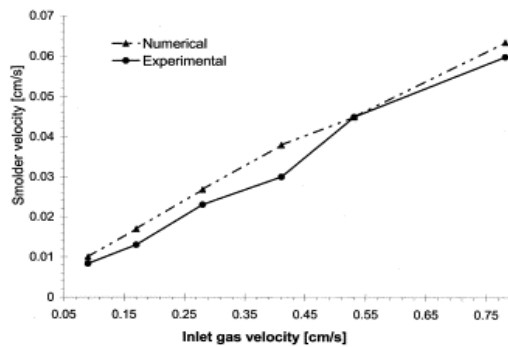

Figure 10. Numerical and Experimental results from Torero and Fernandez-Pello [5]

Following the same explanation as for the temperature increase with higher flows, the velocities increase, because more oxygen is provided to the combustion front, so the peat can react more efficiently and finish faster the reaction in a given position. Then the reaction propagates to the adjacent position and so on.

The decrease of the velocities could be explained with two hypothesis or by a combination of both:

- Since the air flow is high, it has a very big momentum. Therefore, the oxygen instead of stopping in the reaction zone it passes over it. So the actual rate of oxygen consumed by the reaction is smaller, and consequently generating slower velocities.

- The convective heat losses are much bigger with higher air flows, therefore the preheating of the layers ahead of the reaction is less efficient so it takes more time for the material to decompose. Thus, if the material ahead is cold and not enough charred it impossibilities to the reaction to move forward, slowing down the process.

3.1.4 Effect of turbulence.

In Section number 3.2.2, It is derived the equation for Reynolds number for this type of problem. Where Reynolds number is a dimensionless quantity defined as a ratio of inertial forces to viscous forces:

$$R_e = \frac{inertial\ forces}{viscous\ forces} = \frac{\rho v L}{\mu} \tag{11}$$

Where

ρ – Density of the fluid [kg/m³]
v – Kinematic viscosity of the fluid [m²/s]
L – Hydraulic diameter [m]
μ – Dynamic viscosity of the fluid [Ns/m²]

Therefore, Reynolds number quantifies the relative importance of these two forces, defining this way if a flow for given conditions will have a turbulent or laminar behaviour. It is generally assumed that fully laminar flow is developed when $R_e < 10$ and a totally turbulent flow when $R_e > 2000$

Since in this type of experiments it is changed the inlet air gas velocity, this may affect the Reynolds number (Graph 13) and consequently the air flow behaviour inside the pore and interstices of the sand matrix.
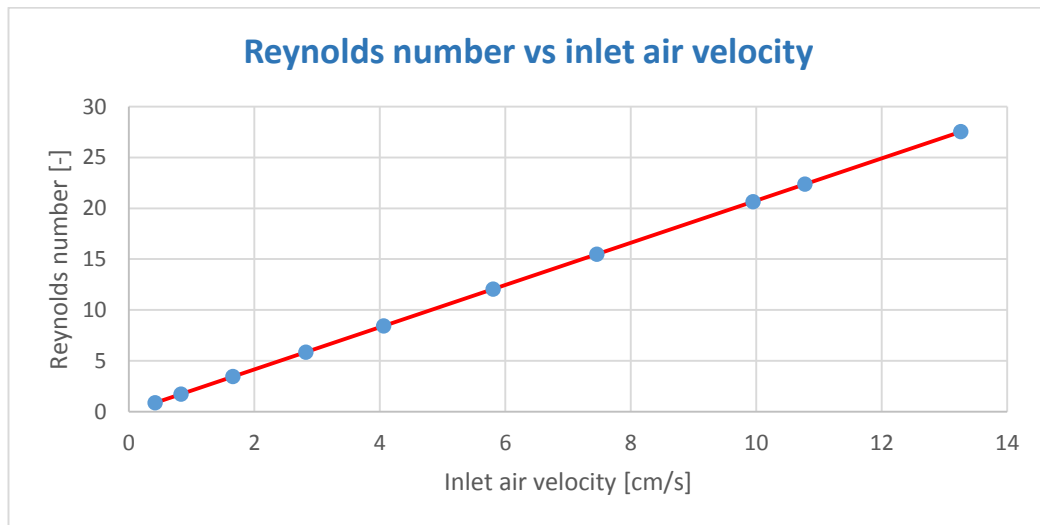
Graph 13. Increase of turbulence represented as the increase of Reynolds number for higher inlet air velocities.

The Reynolds number has a linear dependency of the flow velocity, thus higher flow velocities trigger bigger Reynolds number meaning that the flow becomes more and more turbulent.

Within the range of flows used for the tests of this section, it is observed that Reynolds number varies from 0.86 to 27.53. Hence for an air velocity of approximately 5 cm/s the

flow presents a laminar behaviour inside the porous matrix, while all the higher flows are already in the transition range from laminar to turbulent flow.

The mechanism of how the turbulence may affect the process is by increasing the efficiency of the transport process (transfer of heat and reactive species) due to the eddy mixing in the reaction zone. As these parameters control the propagation velocity, the burning rate is higher in a turbulent environment. [8]

For this case, the effect of turbulence may be very small. Even though it might me another component that influence the temperatures and speed of smouldering propagation.

3.2 Experiments type 2

3.2.1 Temperature analysis.

For this section is done an analysis of the temperatures with different oxygen flows.

The straight output of an exemplar test looks like the graph below. Each curve represents the temperature history by time registered by a given thermocouple. The explanation of the shape of these curves is exactly the same as for Graph 1. The differences are that now there are 24 thermocouples instead of 10, and that the results are more homogenous, because the measurement are taken further from the ignitor where the process is fully developed and closer to steady state.

30% $N_2 \rightarrow$ 4.55 O_2 [g/s·m^2]
total gas velocity 2.17 [cm/s]
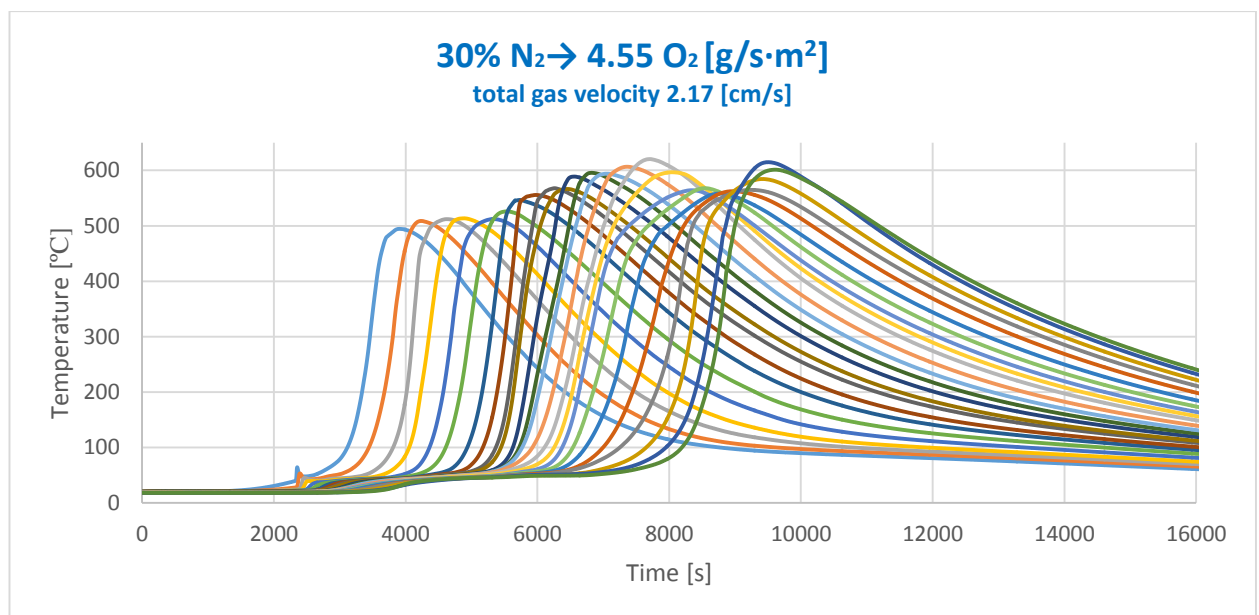
Graph 14. Exemplar output of a test for experiments type-2

After averaging the temperature pics of all the tests which are attached in appendix B, it is possible to observe a trend in the temperature for different oxygen fluxes Graph 15
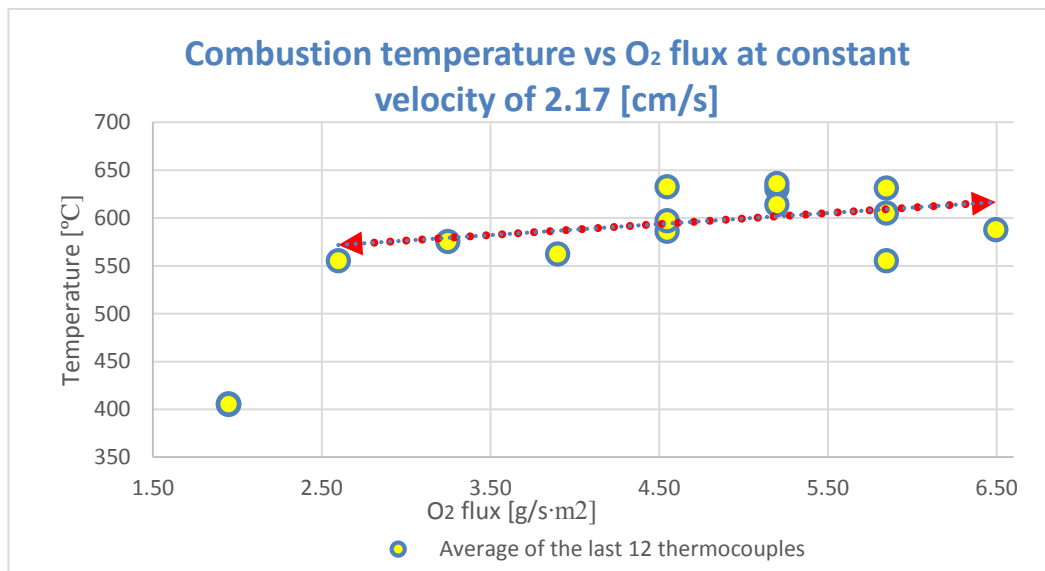
Graph 15. Trend of the smouldering temperature for different inlet oxygen fluxes.

It is detected a small effect on the temperature due to the oxygen concentration. The hypothesis is that the efficiency of the reaction decreases, but the reaction front thickness increases (explained later in this work) Therefore, with smaller concentrations there is more amount of material burning, but at a lower rate. So the increasing amount of material compensates partially the lost efficiency of the combustion; resulting with a small dependency of the temperatures vs oxygen concentration.

Equally to the previous type of experiments, it can be observed that the way of interpreting the results plays a big role, but still for this section it can be concluded that independently of the way of averaging the temperature tend to increase with higher oxygen concentration even though this variation is smaller than expected.
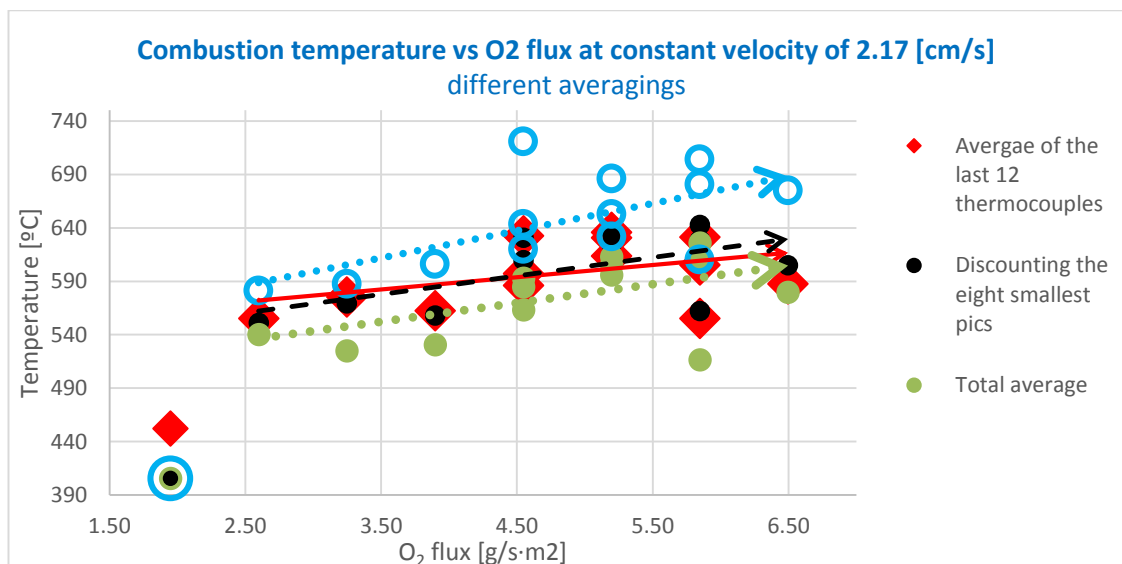
Graph 16. Trend of the smouldering temperature for different inlet air oxygen fluxes and different ways of averaging the temperatures. Information extracted from the tests attached in appendix B

When merging the both variables together (gas velocity and oxygen concentration) it can be created a 3D plot like Figure 11
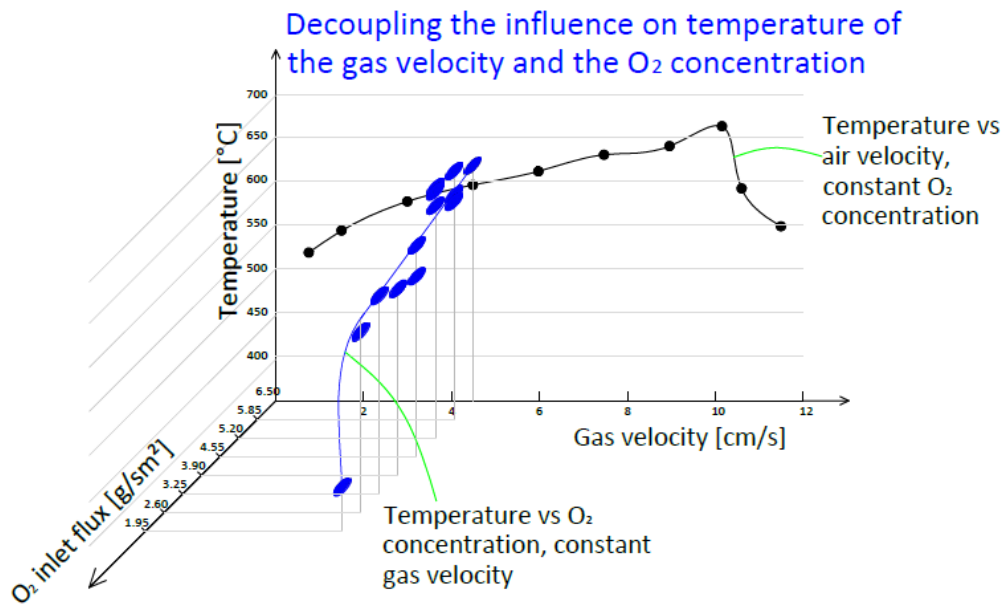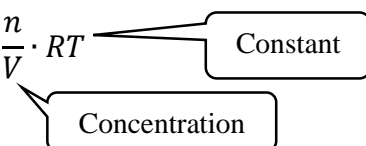

Figure 11. Compilation of the temperature results from experiments type-1 and experiments type-2

This gives place to a discussion about what has actually a bigger influence in the temperatures of smouldering. In the previous section it was concluded that if the amount of oxygen is enough to sustain smouldering, then providing more oxygen is increasing very little the temperatures.

As result it can be concluded that with higher inlet air velocities the temperature increase because of three mechanisms:

- Until some point there is a better preheating of the material ahead of the reaction, allowing the reaction to react easier because the material is already in a higher energy level, and the heat losses to the material around the reaction are lower because the temperature difference is smaller.

- With more air flow, there is also more oxygen flow. Which increases a bit the burning rate resulting in higher temperatures.

- Since there is gas velocity in the analysed system, it is correct to state that there is a pressure gradient inside the column, because any flow needs a pressure difference in order to flow from a higher pressure zone to the lower one. Therefore, it is right to say that the pressure inside the column is bigger than the atmospheric pressure, and as higher is the gas velocity as higher the pressure inside the system. Consequently, the combustion reaction takes place in a pressurized environment.

It is known that for all the reactions where at least one of the reactants is in a gaseous form, the pressure has an effect in the reaction rate [9]. Where higher pressure means higher concentration, and this can be derived from the ideal gas equation:

(12)

$$pV = nRT \quad \Rightarrow \quad p = \frac{n}{V} \cdot RT$$

Constant

Concentration

Where:

p - Pressure
V - Volume
n – Mole umber
R – Ideal gas constant
T – Temperature

So the pressure has an effect on the collision involving two particles. For any reaction to happen, it is essential for the particles to collide. So with higher pressure, there is more particles, and this particles vibrate and move with bigger rates, increasing the probability of collision, and increasing the reaction rate.

Following this hypothesis, now it easier to understand why the temperatures do not vary that much as expected in the experiments type-2. As the inlet gas velocity remains constant for all the tests, this switches off the mechanisms 1 and 3 described before, so the only mechanism left responsible for the increase of temperatures is mechanism 2, which is far to be as effective as the three mechanism working at the same time.

3.2.2 Analysis of the temperature profile curves.

The temperature distribution through the height of the cylinder during the experiment changes as shown in Figure 12. Where the Optimum zone is where the reaction front is localized. For given time, there is a temperature difference from point A to point B. Therefore, there is heat transfer in A-B direction, mainly by conduction and convection (radiation can be neglected).
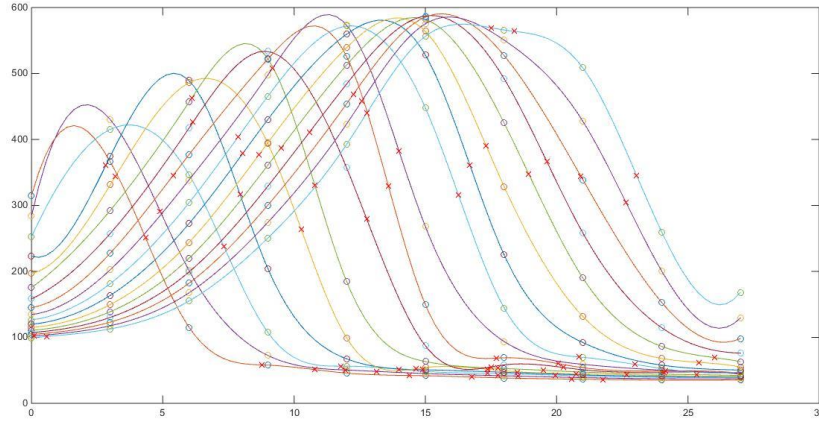
Figure 12. Exemplar output of the temperature profile curves for experiments type-1

The Idea is to analyse the effects of conduction and convection separately, and check how they influence the temperature distribution inside the cylinder.

For the convection mechanism, it is considered that the pores between the grains of sand constitute a net of very fine pipes. This assumptions is derived from the reference [10]

From the book "*Introduction to the grain technology*" [10] a general equation for turbulent and laminar flow is developed. It is based on extensive experimental data covering a wide range of size and shape of particles. Ergun (1952) suggested the following general equation for any flow condition through a randomly packed bed of spherical grains of diameter x [10]:

$$\frac{(-\Delta_p)}{H} = 150 \frac{\mu U}{x^2} \frac{(1-\varepsilon)^2}{\varepsilon^3} + 1.75 \frac{\rho_f U^2}{x} \frac{(1-\varepsilon)}{\varepsilon^3} \tag{13}$$

$$\begin{pmatrix} laminar \\ component \end{pmatrix} \quad \begin{pmatrix} turbulent \\ component \end{pmatrix}$$

Where:

$(-\Delta_p)$ – Frictional pressure drop across a bed depth
H – Bed depth
U – Superficial fluid velocity through the bed →fluid volumetric flow rate/ cross section are of the bed
μ – Fluid viscosity
ε – Voidage or void fraction of the packed bed
x – Diameter of the particle
ρ_f – Fluid density

This Ergun's equation combines the components of the laminar and turbulent flow for the pressure gradient. The first term dominates under laminar conditions. This term is directly derived from the Hagen-Poiseuille equation for laminar flow through a tube:

$$\frac{(-\Delta_p)}{H} = \frac{32\mu U}{D^2} \tag{14}$$

Where D is the tube diameter. Adjusting this equation to a packed bed by considering many tubes of equivalent diameter, tortuous path through equivalent length and the actual velocity through the interstices, the Hagen-Poiseuille equation transforms into Carman-Kozeny equation:

$$\frac{(-\Delta_p)}{H} = 180 \frac{\mu U}{x^2} \frac{(1-\varepsilon)^2}{\varepsilon^3} \tag{15}$$

Which is the laminar component of Ergun's general equation. The constant 180 changes to 150 probably due to the difference in shape and the packing of the particles.

Laminar flow means that the pressure gradient increases linearly with superficial fluid velocity and it is independent of the fluid density.

On the other hand, turbulent flow appears when the second term of the general equation dominates, then the pressure gradient increases as the square of the superficial fluid velocity and it is independent of the fluid viscosity. [10]

Thus, for this type of problem the Reynolds number is defined as:

$$Re^* = \frac{xU\rho_f}{\mu(1-\varepsilon)} \tag{16}$$

Where $Re^* < 10$ means that the flow is completely laminar, while a fully developed turbulent flow exists when $Re^* > 2000$.

With the previous information it is possible to calculate the Reynolds number for the setup of experiment type-2

Parameter	value	Unit
x	0.002	[m]
U	0.0216	[m/s]
ρ_f	0.6	[kg/m^3]
μ	305,8·10^{-7}	[Ns/m^2]
Sand density	1602	[Kg/m^3]
Volume of the sand	0.0054	[m^3]
Amount of sand	7	[kg]
ε	$\frac{7}{0.0054 \cdot 1602} = 0.812$	[-]

$$Re^* = \frac{0.002 \cdot 0.0216 \cdot 0.6}{305.8 \cdot 10^{-7}(1 - 0.189)}$$
$$= 4.49 \, [-]$$

Table 3. Parameters to calculate Reynolds number for the flow in experiments type-2

Laminar flow

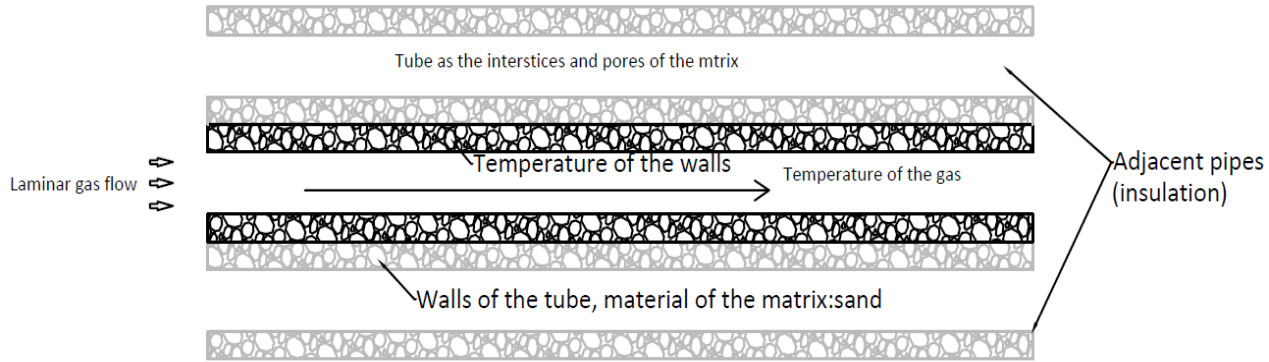Summing up, the problem to solve is as presented in Figure 13.

Figure 13. Scheme of the convection problem in a porous matrix.

It can be assumed that the pipe is thermally insulated, since it is surrounded with other pipes that are submitted under the same process, so they are also heated up. Consequently, in a given section there is no temperature difference between the pipes surfaces so there is no heat transfer between them. So the heat losses can be neglected and the problem can be approached as thermally insulated.

The equation for local heat flux by convection is:

$$q'' = h(T_s - T_\infty) \tag{17}$$

Where:

h - local convection coefficient

T_s – Temperature of the solid

T_∞ - Temperature for the gas

To find the temperature distribution of the pipe, Eq. (17) should be solved for every point of the tube, since: $T_s = T_\infty + \frac{q''}{h}$. However, T_∞ and q'' are unknown as well.

For future work, it is proposed to solve numerically the energy balance for every finite element of the gas and solid. Additionally, the experiments could be run with a new thermocouple design (Figure 14), that would measure only the temperature of the gas phase. This way the temperature difference for a given point could be checked, as well as if the process works in thermal equilibrium.
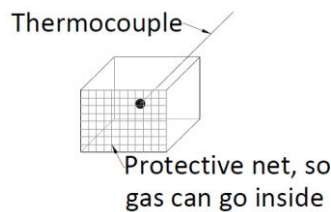

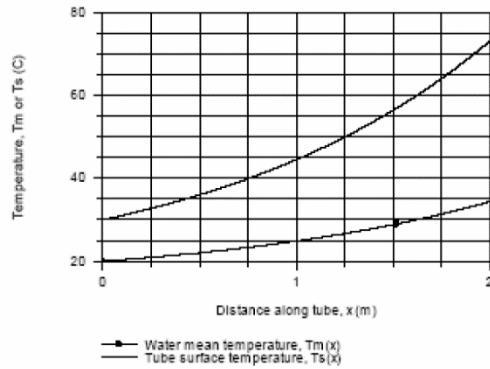*Figure 14. Proposed thermocouple design to measure the gas phase*

Figure 15. Temperature distribution along the pipe, in the pipe surface and the fluid. [13]

In literature similar problems to this were solved, also by using numerical integration in IHT software (Internal Heat Transfer software). The results of this problems always present similar shapes of a concave function, like in the example in Figure 15Figure 15.

Also from theory it is known that by conduction the temperature distribution through the thickness of a material, from a higher to a lower temperature present a concave form which asymptotically drops to the ambient temperature [12], as shown in Figure 16.
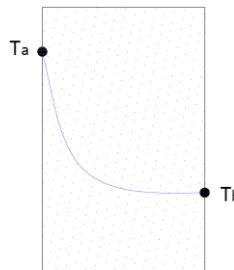

Figure 16. Temperature distribution through a solid

Therefore, the overall shape of the temperature profile is the addition of the effect of the conduction plus the convection, and because both of this mechanism present a concave profile, the result of the sum is also concave.

As the results of the tests present inflection points in the temperature profiles, meaning that the curves change from concave to convex. It implies, that in the convex zone it is not a heat transfer phenomenon which is occurring, so by discard, it has to be the heat generation zone, which is equivalent to the reaction zone.

Because of this conclusions all the inflection points were calculated assuming that the interval between them is the thickness of the reaction front, in 3.2.3 are presented the results of this calculations already in a front-thickness form.

3.2.3 Analysis of the thickness of the reaction front.

In the graph below it can be observed that the thickness of the reaction front tends to increase with lower oxygen concentration. The mechanism of this phenomena could be explained with the following assumptions:

Combustion front thickness vs O₂ inlet flux for constant flow velocity 2.17 [cm/s]
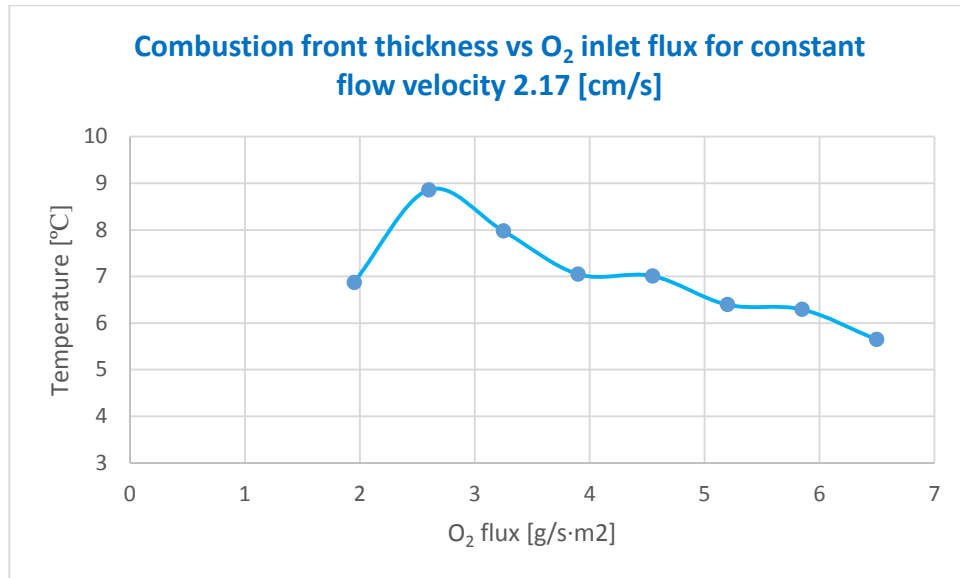
Graph 17. Compilation of the front thickness for all the tests performed for experiments type-2

- Since the flow is constant, the heat is equally transported ahead of the reaction by convection, so the leading edge of the reaction zone can propagate forward anyway because the material is preheated and with good conditions to react.

- While the front of the reaction zone is moving forward, the rear side is not fully combusting because the oxygen is limited, so it will take more time to it to finish burning, causing a delay of the last line of the combustion zone. This way the thickness of the reaction zone increases.

- With very low oxygen concentrations, we can see that the thickness starts to decrease again, this may be due to the fact that all the oxygen is consumed in the reaction zone. Consequently, the unreacted oxygen is not enough to start reacting with new material. So the front remains in the same position until everything is burned and then it can start consuming new portions of material, In this case the reaction is much more localized, because the amount of oxygen is so low that it does not give a chance the reaction to spread. This matches with Graph 19 where the velocities do not change any more under certain oxygen flow.

This phenomena can occur because smouldering has a very wide range of efficiencies at which can combust. Consequently, with lower oxygen concentrations it is possible to have more material burning but less efficiently. This translates into thicker combustion fronts but burning at a lower rates.

For the end of this section it is also important to mention that the reaction zone was not normally reaching steady state for higher propagation velocities. As shown in Graph 18.

Where the beginnings of the tests present a quite irregular value for the thickness and later they seem to stabilize. Optimally, there should be taken into account only the values that are within steady state, but this was impossible since for many tests the column was too short for the reaction to reach this state. Even if the averaging presents a clear trend presented in Graph 17, this tests should be repeated in a longer column to prove that the conclusions in this work are based in a real physical behaviour.
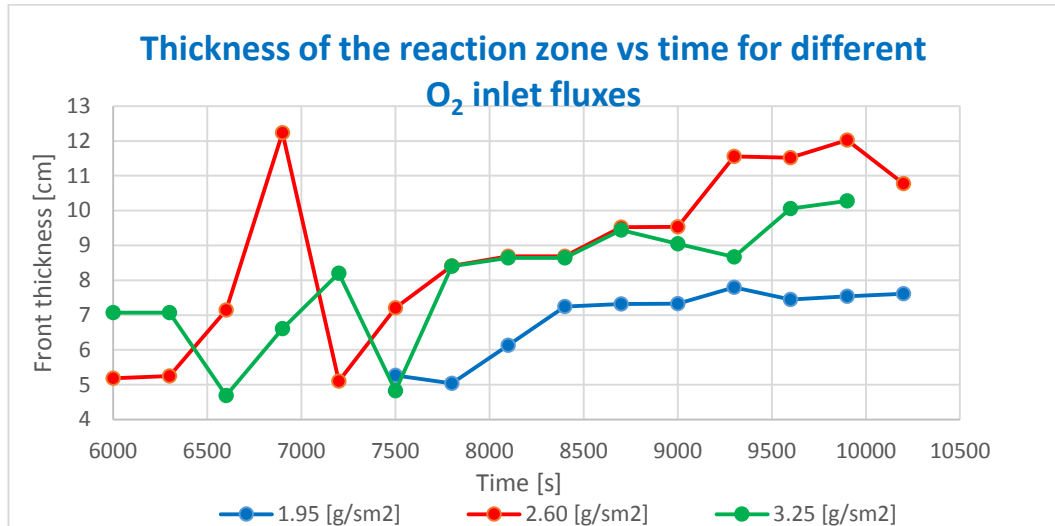
Graph 18. Front thickness vs time for exemplar tests of experiments type-2.

3.2.4 Analysis of the velocity for different oxygen concentration:

In this section it is discussed how the oxygen concentration affects the propagation velocity. Same as previously, what is analysed is the speed of traveling of the thermal wave at 500 ºC, obtaining the results presented in Graph 19.
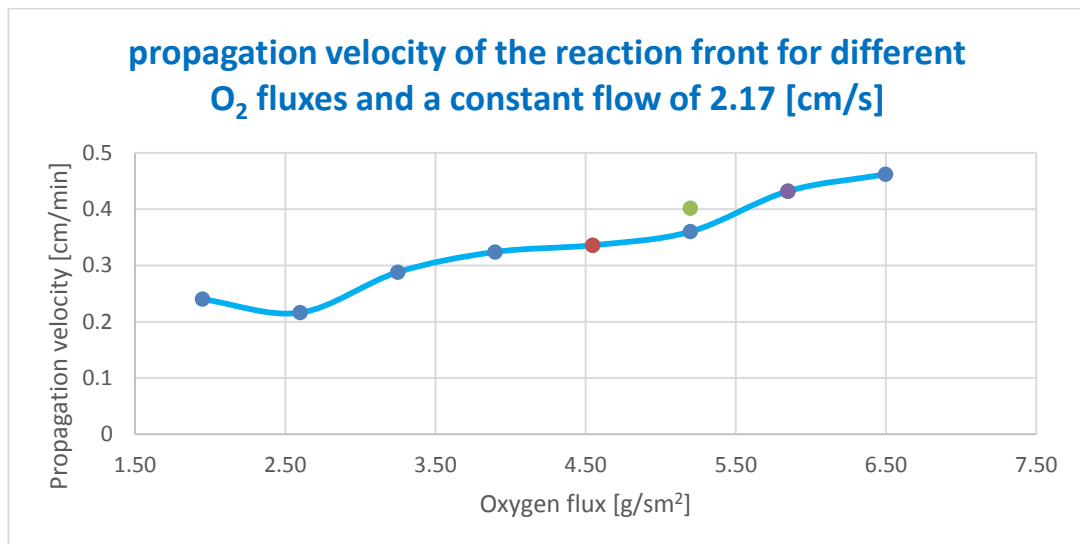
Graph 19. Compilation of the results of all the tests of experiments type-2 for the propagation velocity for different inlet oxygen concentrations.

Following the same explanation as for the temperature profile section: For having propagation two conditions have to be met:

- The material has to be enough preheated, so it decomposes in char and pyrolysis gases making possible the reaction to happen.

- Available oxidizer to react with the pyrolysis gases.

Therefore, in this case the first condition is met, since the total gas flow remains constant, it can be assumed that the preheating of the material ahead of the reaction is equal for all cases, so the rate of generation of char also.

Then, the condition two is the responsible for slowing down the system. Since there is less oxygen available, the char has to wait longer for enough oxygen to come in order to create a flammable mixture and then react. This "waiting time" is the responsible for decelerating the smouldering velocity.

Again the velocities follow the behaviour of the temperatures, decreasing with lower inlet oxygen fluxes.

3.2.5   Analysis of the Damköhler number.

Other way for explaining the behaviour of smouldering that was found out for this type of experiments is by analysing the non-dimensional Damköhler Number [Da]. This number corresponds to a ratio between chemical time scales and turbulent time scales of the flow. It measures how important is the interaction between chemistry and turbulence:

$$D_a = \frac{Characteristic\ turbulence\ time}{Characteristic\ chemical\ time} = \frac{\tau_T}{\tau_C} \frac{[s]}{[s]} \tag{18}$$

If Da << 1 then turbulence is much faster than chemistry

If Da >> 1 then chemistry is much faster than turbulence.

According to the reference [6], which also refers to forward smouldering of peat, the Damköhler number in solid phase is defined as:

$$D_a = \left(\frac{L}{S}\right)/\tau \tag{19}$$

Where:

L - Characteristic thickness of the smouldering front.
S – Smouldering spread rate.
τ – Characteristic reaction time $\rightarrow$ inverse of the reaction rate.

From the experiments all these variables can be estimated:

L – Given by the previous calculated inflection points that define the front thickness

S – Previous calculated velocity of the thermal wave.

τ – It is known that 7 kg of sand-peat mixture occupies 35 cm of the height of the cylinder.

Then, with the velocity of the propagation front it can be calculated how long it takes the

reaction to consume all the peat along this height, giving this way the reaction rate, thus the characteristic reaction time.

In the following table are all the values extracted from the experiments needed to define the Damköhler number for each type of test with the different oxygen fluxes.

Oxygen flux [g/s·m²]	Characteristic thickness of the smouldering front [cm]	Smouldering spread rate [cm/s]	Time to react with all the peat in the column [s]	Reaction rate [g/s]	Characteristic reaction time [s/g]	D_a [-]	$1/D_a$ [-]
6.50	5.65	0.0077	4545.45	0.0616	16.23	16.23	0.02214
5.85	6.29	0.0072	4861.11	0.0576	17.36	17.36	0.01986
5.20	6.39	0.0060	5833.33	0.0480	20.83	20.83	0.01955
4.55	7.01	0.0056	6250.00	0.0448	22.32	22.32	0.01783
3.90	7.05	0.0054	6481.48	0.0432	23.15	23.15	0.01773
3.25	7.98	0.0048	7291.67	0.0384	26.04	26.04	0.01567
2.60	8.86	0.0036	9722.22	0.0288	34.72	34.72	0.01411
1.95	*6.87*	*0.0040*	*8750.00*	*0.0320*	*31.25*	*31.25*	*0.01819*

Table 4. Estimated values from all the tests of experiments tyoe-2 needed to calculate the Damköhler number.

Taking the values from Table 4 the Damköhler number can be calculated for all the tests giving plave to Graph 20 that shows the trend of the Damköhler number versus the oxygen flux:
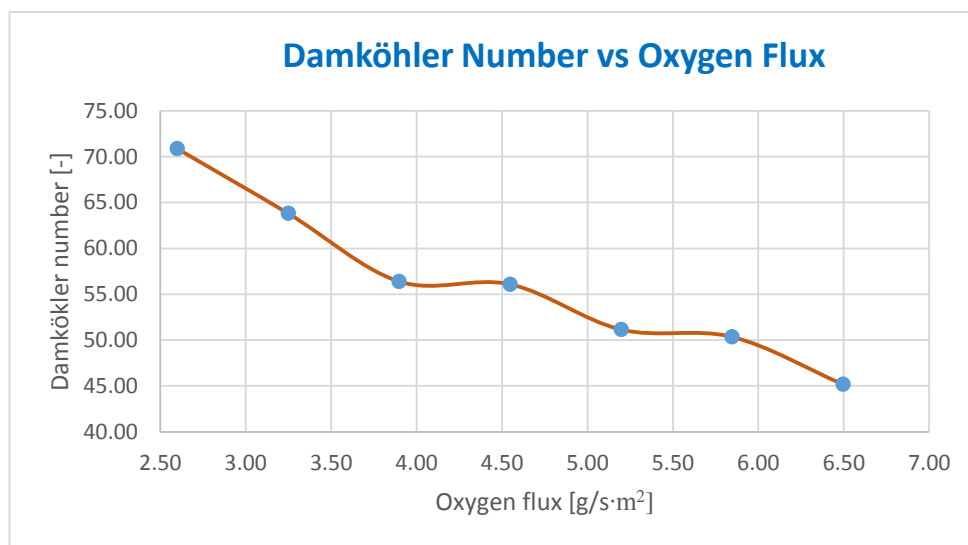
Graph 20. Damköhler number for all the tests of experiments type-2.

As it can be observed, for all the different fluxes of oxygen, the Damköhler number is much greater than 1. Therefore the reaction rate [11] is much greater than the diffusion rate distribution, so diffusion is slowest and its characteristics dominate the process while the reaction is assumed to be instantaneously in equilibrium.

Then it makes sense that with lower oxygen concentration the Damköhler increases. So the burning rate will get lower while the influence of the turbulence will lead more and more all the process.

From here it can be deduced again that [14] at high Damköhler numbers, the oxygen supply rate becomes the rate-limiting step, so by lowering the oxygen concentration, the smouldering velocity decreases. Or in other words: for large Damköhler numbers, the reaction is so fast that its effects of finite gas-phase chemical kinetics become unimportant. Consequently, it is the heat transfer from the gas to the solid that controls the spread of the process.[15]

From previous models that describe the wind-aided flame spread under oblique forced flow [15] it was also calculated the Damköhler number as presented in Figure 17. This figure presents the reduction of the flame spread velocity due to finite rate effects, represented by the corrected nondimensional spread velocity, $\overline{\Omega} = \Omega/\Omega_{BS}$, as a function of the modified

Damköhler number $\overline{D}$ defined as $\overline{D} = \frac{4}{T_f q}\left(\frac{ST_f^2}{qT_a}\right)^3 De^{-T_a/T_f}$. <u>Where Ω_{BS} is equal to 5.77, 9.13 and 16.7 for $Y_{O\infty}$ equal to 0.18, 0.23 and 0.33, respectively.</u>
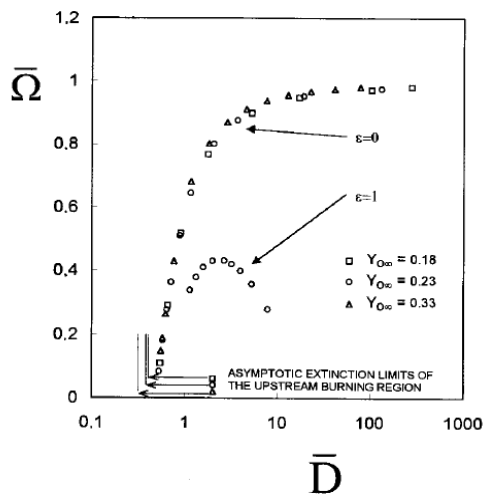

Figure 17. Results from reference [16]
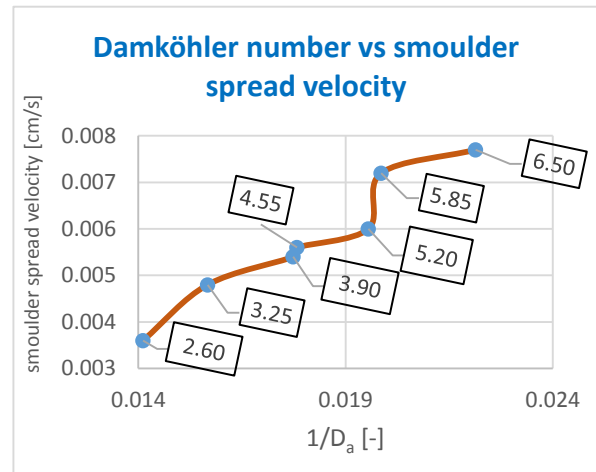
Graph 21. Damköhler number for different smouldering velocities obtained with the data from experiments type-2

It is difficult to compare the figure from the model with the graph showing the values from the experiments (that presents the invers of Da to be more comparable with the model), since one concerns a flaming problem and the other one smouldering. However, there are some similitudes in the combustion behaviour. For both cases the velocity presents an increase respect to the Damköhler number decrease as well as there is an influence of the mass flux (for Graph 21, the oxygen flux [g/s·m2] is annotated next to each label). Where the

increasing amount of available oxygen leads to smaller Damköhler numbers and gives place to higher velocities for both cases.

 For future work, it would be recommended to perform more tests and check if the results can validate a similar model like the developed for the flaming case, but for smouldering.

3.3   Experiments type-3

So for this section were repeated the tests from the previous experiments and what was measured was the concentration of the unreacted oxygen..

Graph 22 presents how the concentration of the unreacted oxygen varies along the tests with different inlet oxygen fluxes.
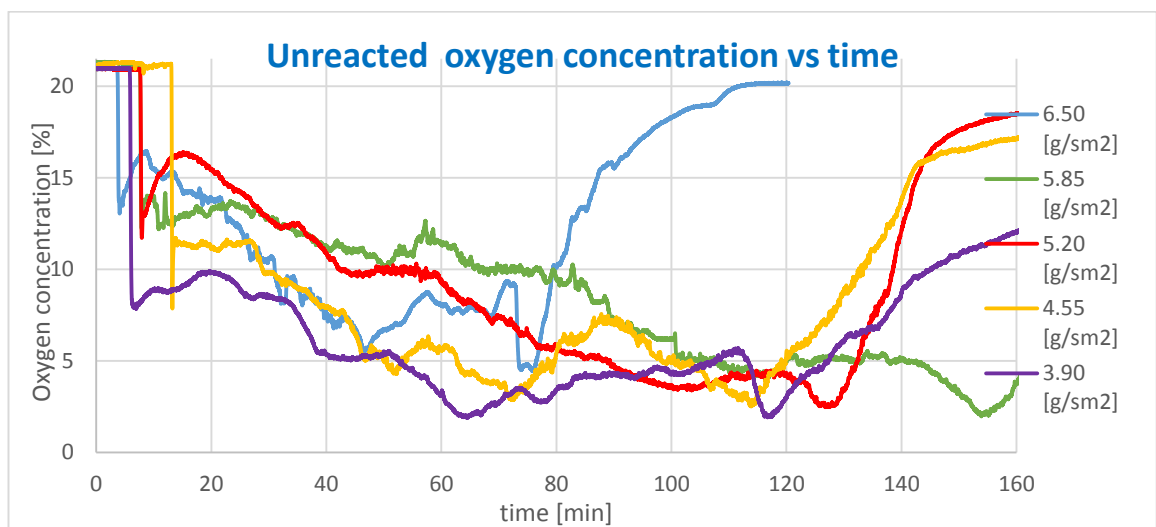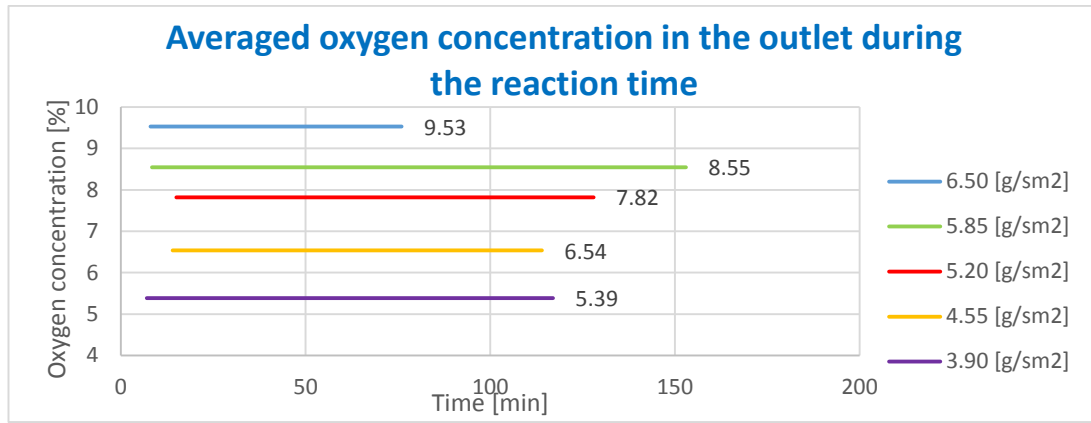

Graph 22. Outlet oxygen concentration vs time, for different inlet oxygen concentration for experiments type 3.

 Since each test has a different duration, different burning rate and additionally the concentration of the unreacted oxygen presents many fluctuations it is difficult to define a trend depending on inlet oxygen flux. Even though, it can be observed that generally the curves that represent the tests with higher inlet oxygen flux are above the curves of the tests with smaller oxygen fluxes.

Approach 1: averaging over all the duration of the reaction.

In order to make the results more readable, it is taken into account only the range where a fully developed reaction appears. It means from the first drop of oxygen concentration until the beginning of the reaction decay, that translates into arise of the oxygen concentration in the outlet. So from the first until the last minimum of each curve. Then it is made an average of all the concentrations for every time step in this range, giving as a result the following graph:

Graph 23. Averaged oxygen concentrations in the outlet for the tests of experiments type-3

Here it can be clearly seen that for lower inlet oxygen fluxes, there is also a lower oxygen concentration in the outlet. Therefore, here is the starting point to calculate the percentage of consumed oxygen for each test.

Inlet oxygen flux [g/sm²]	Inlet oxygen concentration [O₂%]	Outlet oxygen concentration [O₂%]	Consumed oxygen [%]
6,50	21	9.53	0.55
5.85	18.9	8.55	0.55
5.20	16.8	7.82	0.53
4.55	14.7	6.54	0.56
3.9	12.6	5.39	0.57

Table 5. Oxygen balance in the apparatus for experiments type-3

With this approach it can be observed that smouldering always consumes a similar percentage of the available oxygen. That would encourage to think that the process is not oxygen limited. However, this suggestion contradicts the facts that smouldering extinguishes below certain oxygen concentration of around 3% O_2.
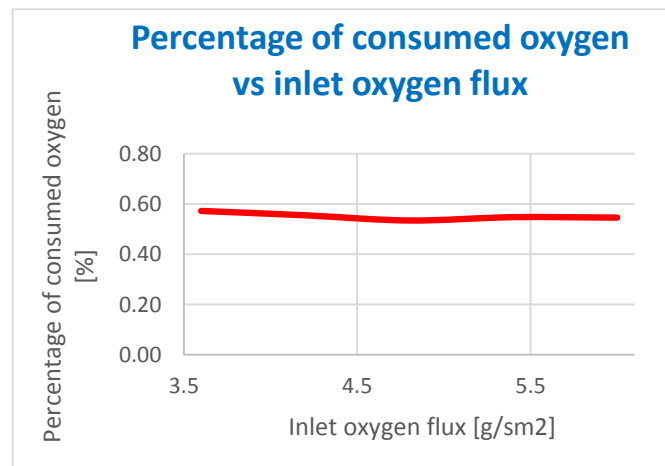
Graph 24. Percentage of consumed oxygen for all the tests in experiments type-3, taking into account all the period of the reaction process.

Other hypothesis is, that the total gas velocity is still so high, that it does not allow the oxygen to stay in the reaction zone. So even if the burning region can potentially use more oxygen, this needed oxygen just travels through it.

Even if the gas-analyser could not measure the CO and CO_2 concentrations, it is logical to assume that with less oxygen available the production of CO will increase while the generation of CO_2 will decrease. Since CO needs half of the oxygen, it somehow compensates the fact that there is less oxygen in the inlet, but also less oxygen is used in the reaction because the spices generated are different.

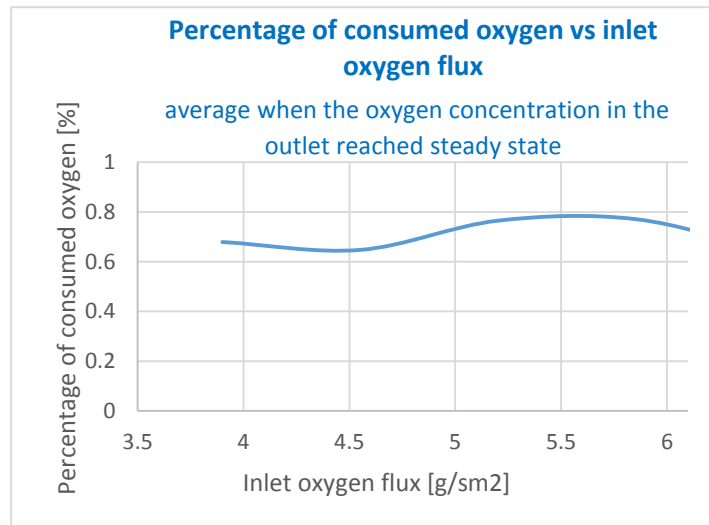*Approach 2: Averaging when the outlet oxygen concentration is in "steady state"*

It is important to remember that initially the pores of the matrix are filled with air, where the oxygen concentration is relatively high of about 21%. Probably the combustion firstly reacts with the air in the pores, and then with gas from the diffuser. In Graph 22 it can be appreciated that for all the tests, first the concentration have a decay phase, and when all the air is blown out of the pores the concentration stay in more or less in the same level.

Hence, in this approach the average will be done from the point where it is subjectively considered that there is no more of the initial air in the pores.

Inlet oxygen flux [g/sm^2]	Inlet oxygen concentration [O_2%]	Outlet oxygen concentration [O_2%]	Consumed oxygen [%]
6,50	21	7.58	0.64
5.85	18.9	4.32	0.77
5.20	16.8	3.95	0.76
4.55	14.7	5.18	0.65
3.9	12.6	4.04	0.68

Table 6. Oxygen balance taking into account only the time when the initial air in the pores has been blown out.

This calculation just differ from approach 1 by showing a bit higher consumption of oxygen, but still the trend looks quite linear, meaning that smouldering is consuming always a similar percentage of Oxygen independently of the oxygen flow.

Percentage of consumed oxygen vs inlet oxygen flux

average when the oxygen concentration in the outlet reached steady state

Graph 25 Percentage of consumed oxygen for all the tests in experiments type-3, taking into account the period when the oxygen concentration in the inlet is in "steady state"

Independently of the used approach, the percentage of consumed oxygen is almost constant. On one hand, this discovery proves the previous assumptions from section 3.2.3, saying that the consumption rate of oxygen is lower for smaller oxygen fluxes in the inlet. Implying a smaller burning rate.

But on the other hand, it remains unknown the reason why the reaction does not use more of the oxygen available if it is in an oxygen-limited condition.

4 Conclusions

For experiments type-1 it is proved that the temperatures and the smoulder spread speed behave unlikely when increasing the air flow. For both parameters it is observed a decay for very high inlet velocities mainly due to the cooling effect.

For the experiments type-2 it is proved that the method of using IP of the temperature-profile curves as a reference to establish the front thickness is more accurate than the ordinary approach. Even though, this methodology should be improved since it is difficult to establish the real position of the IP. This experiments show that there is a small variation of temperatures depending on the oxygen concentration, and by analysing the thickness of the reaction front it is concluded that this phenomenon is due to the fact that with lower oxygen concentrations, the reaction zone is bigger but the burning rate is smaller, therefore this two variables compensate the overall heat generation.

Experiments type-3 demonstrate that the assumptions for experiments type-2 were valid, since the analysis of the exhaust gases indicate that the consumption of oxygen is at lower rate with lower inlet oxygen fluxes. But it is not well understood why smouldering always consumes a similar percentage of the oxygen, independently of the oxygen that is available.

For future work, it is strongly recommended to use the automatized mass flow meters instead of the conventional flow meter. Because the first one assures with big accuracy the actual amount of mas flowing into the system.

Also it is recommended to perform the experiment in longer tubes, since the process always needs some space to reach steady state.

Since the experiments type-3 resulted with completely unexpected results, they should be repeated several times to validate them. As well as the thickness of the reaction fronts for experiments type-2 should be recalculated only taking into account steady state (thus, longer columns are needed)

It would be also very interesting to try to measure the temperatures of the solid and gas phase separately, and check if the experimental data match with the theory about the temperature distribution in a porous matrix heated by a hot flow that flows through it.

Acknowledgements

I would like to show my gratitude to Dr Paolo Pironi, for giving me the best support while working in the laboratory. As well as for his finest guidance with the interpretation and understanding of the results.

In addition, I thank to my supervisor; Dr Rory Hadden, who always pushed and broadened my horizons in all the meeting, making out of this thesis much more than I expected.

References

[1] G. Rein, "Smouldering Combustion Phenomena in Science and Technology", *International Review of Chemical Engineering, Vol 1, pp 3-18. Jan 2009..*

[2] N. A. Moussa et al. "Mechanism of Smouldering of Cellulosic Materials", *Massachusetts Institute of Technology, Cambridge, Massachusetts.*

[3] D.C. Walther et al, "Smolder Ignition of Polyurethane Foam: Effect of Oxygen Concentration", *Fire Safety Journal 34 (2000) 343-359.*

[4] T.J. Ohlemiller, "Smoldering Combustion", *Fire Dynamics, Section Two, Chapter 9.*

[5] S. V. Leach et al. J. L. Torero, "Kinetic and Fuel Effects on Forward Smoldering Combustion", *Combustion and flame 120:346-358 (2000).*

[6] X. Huang, G. Rein, "Smouldering Combustion of Peat in Wildfires: Inverse Modelling of the Drying and the Thermal and Oxidative Decomposition Kinetics", *Combustion and Flame 161 (2014) 1633-1644.*

[7] S. E. Page, F. Siegert, J.O. Rieley, *Nature 420 (2002) 61-65*

[8] Dougal Drysdale, "An Introduction to Fire Dynamics" *Wiley, third edition.*

[9] http://www.chemguide.co.uk/physical/basicrates/pressure.html

[10] Martin J. Rhodes, "Introduction to Particle Technology" *Wiley, second edition.*

[11] http://web.mit.edu/beh.430/www/BEH430/Extras/Week2/A%20word%20about%20Damkohler%20numbers3.htm

[12] Frank P. Incropera, David P. DeWitt "Fundamentals of Heat and Mass Transfer"

[13] Frank P. Incropera, David P. DeWitt "Fundamentals of Heat and Mass Transfer. Solution Manual"

[14] S. V. Leach. Et al. "Convection, Pyrolisis and Damkohler Number Effects on Extinction of Reverse Smoldering Combustions", *Twenty-seventh Symposium (International) on Combustion/The Combustion Institute, 1998/pp, 2873-2880.*

[15] J.M. Tizon et al. "Wind-Aided Flame Spread Under Oblique Forced Flow", *Universidad Politecinca de Madrid, E. T. S. I. Aeronauticos, Madrid, Spain.*